Applied Energy 356 (2024) 122426

Contents lists available at ScienceDirect

Applied Energy

journal homepage: www.elsevier.com/locate/apenergy

A market-based real-time algorithm for congestion alleviation incorporating EV demand response in active distribution networks ☆

Mohan Menghwar [a], Jie Yan [a,*], Yongning Chi [b], M. Asim Amin [c], Yongqian Liu [a]

[a] North China Electric Power University, School of New Energy, 102206, Beijing, China
[b] China Electric Power Research Institute, Renewable Energy Center, Beijing, 100192, China
[c] Department of Electrical, Electronics and Telecommunication Engineering and Naval Architecture, University of Genoa, Genoa, I-16145, Italy

ARTICLE INFO

Keywords:
Real-time congestion management
Demand response
Lyapunov optimization
EV charging scheduling
Market-based mechanism
Distributed energy resources

ABSTRACT

The dynamic charging behavior of electric vehicles (EVs) is causing frequent line-overloading problems and serious power security issues. Controlled and smart charging mechanisms for EVs incorporating demand response (DR) may provide significant operational flexibility to the grid operators and reduce charging costs for EV users. However, controlling EV charging may cause inconvenience to individual EV users. A market-based mechanism is proposed in this research work that allows EV users and households to participate in the network congestion alleviation DR program online while maintaining the power quality. Consumers submit their charging requirements (e.g., charging power and charging deadlines) and load curtailment tolerances to the aggregator. The aggregator is an entity assumed to have a long-term contract with the distribution system operator (DSO) and regularly receives network congestion information on behalf of retail energy users. Lyapunov optimization (LO) framework is used to reschedule the EVs, and household loads using DC optimal power flow (DCOPF) to get the dynamic congestion cost signal (CCS). The developed strategy is tested on a modified IEEE 33-bus radial active distribution network (ADN). Simulation results illustrate that the designed algorithm is promising in mitigating network congestion by ensuring significantly fewer violations of network constraints (i.e., line limits) both in terms of capacity and frequency. It also results in less energy cost as compared to other benchmark algorithms, e.g., greedy algorithm, and provides a guarantee of meeting EV charging, and flexible household loads' (FHL) delay tolerance constraints. The average curtailment ratio of FHL and the service delay for EV-charging requests are converged to the user-defined limits, i.e., 0.25 for curtailment ratio tolerance and 10 times-lots for EV service delay. Unlike other counterparts, the developed algorithm is especially suitable for real-time applications as the per-slot average computational cost is negligible, i.e., 0.55 s.

1. Introduction

The need for the decarbonized society has triggered widespread curiosity in the use of renewable energy resources (RES). The global renewable share of the power generation mix is increasing faster than the power demand itself [1]. In addition, rapid electrification of the transport sector has already started affecting the normal grid operation. High penetration of RES and other distributed energy resources (DER) accompanying inherent spatio-temporal intermittency at both the supply and demand side. This may lead to severe grid reliability issues [2], and the end-users are also reshaping their roles to attain prosumer status. Prosumers are the end-users equipped with active DERs, such as small-sized renewable generators and energy storage systems (ESSs). EVs can offer great flexibility in terms of supply and demand [3]. Contrarily, if the prosumer potential is not utilized wisely, it may lead to severe grid reliability issues, such as network congestion [4].

Consequently, to make the exploitation of RES and other DERs sustainable in the long term, it necessitates the development of strategies that may hedge against network congestion and other grid operational challenges. Increasing adoption of DERs, due to government promotions in Europe, the US, China and other parts of the world [5] poses a great risk of reverse power flows in the ADN. It results in operating patterns not considered during planning, design, and protection studies of traditional congestion management approaches [6]. One simple way

☆ This work is supported by the project "National Key Research and Development Program of China, Research on Human-Source-Load-Carbon Synergy Optimization Technology for Carbon Neutral City Energy System Driven by Population Trajectory Big Data" under grant 2022YFE0117600.

* Corresponding author.
E-mail addresses: mohan22@ncepu.edu.cn (M. Menghwar), yanjie@ncepu.edu.cn (J. Yan), chiyn@epri.sgcc.com.cn (Y. Chi), asim.amin@edu.unige.it (M. Asim Amin), yqliu@ncepu.edu.cn (Y. Liu).

https://doi.org/10.1016/j.apenergy.2023.122426
Received 14 September 2023; Received in revised form 14 November 2023; Accepted 24 November 2023
Available online 5 December 2023
0306-2619/

Nomenclature

t, a, e	Indices for time-slots, aggregators & EVs
t^{con}, t^{dep}	EV connection and departure time-slot
$t^{\min}, t^{tol}$	Min. & tolerated time-slot for EV charging
$p^{\max}_{e,a}$	Maximum EV charging power
$P^{ch}_{e,a}$	Total Requested charging energy
$p^{ch}_{e,a}$	Charging energy in a time-slot
$P_{e,a}$	Supplied charging energy in a time-slot
T^{ch}, T^{min}	Set of complete & min. charging time-slots
τ	Index for intermediary time-slots
P^{en}_a	Energy supplied to all EVs in a time-slot
P^{sh}_a	Shifted charging energy
$SOC^{dep}_{e,a}$	SOC level at the departure time-slot
$SOC^{con}_{e,a}$	SOC level at the connection time-slot
$SOC^{min}_{e,a}$	Minimum SOC level of EV battery
$SOC^{max}_{e,a}$	Maximum SOC level of EV battery
c^{en}_a, c^{cong}_a	Energy consumption and congestion cost
c^{sh}_a, c^{curt}_a	Energy shifted and curtailed cost
μ^{ene}, μ^{cong}_b	Consumption and congestion per unit rate
μ^{LMP}_b	LMP at bus b
ψ, ω, λ	Lagrangian function and multipliers
k, b, d	Indices for branch, bus & delay-tolerance
η_b	Energy dispatch cost at bus b
GSF_{k-b}	Generation shift factor related to k-b
μ^{loss}_b	Loss component of LMP
α_{sh}, β_{sh}	Shifted charging penalty coefficients
$\alpha_{curt}, \beta_{curt}$	Curtailed FHL penalty coefficients
c^{dso}	Cost associated to DSO problem
G_{min}	Generation capacity lower limit
G_{max}	Generation capacity upper limit
ζ, γ, ξ	Virtual queues trade-off coefficients
p^g_b, p^d_b, p^{chl}_b	Nodal generation, demand & critical load
L^{curt}_a, L^{flex}_a	Curtailable and flexible load under “a”
$L_a, L^{\max}_a, L^{crit}_a$	Supplied, Max. & critical load under “a”
$R_{d,a}, O_{d,a}, I_{d,a}$	EV Charging request queues
$M_{d,a}, Z_{d,a}$	Delay aware virtual queues
V	Lyapunov cost trade-off parameter
ϵ	Delay control finite +ve parameter
D	Set of delay aware queues
Θ, ϕ	Queue backlog & QoP coefficient
B	Cost-procurement trade-off parameter

Abbreviations

V2G	Vehicle to Grid
FHL	Flexible household load
CCS	Congestion cost signal
ADN	Active distribution network
DSO	Distribution system operator
RES	Renewable energy source
DER	Distributed energy resources
LMP	Locational marginal price
RCM	Real-time congestion management
TTC	Transformer Tap Changer
QoP	Quality of power
CHL	Critical household load
DR	Demand response
DCOPF	DC optimal power flow
LO	Lyapunov optimization
ICT	Information and communication technology
SOC	State of charge
EV	Electric Vehicle
ATC	Available Transfer Capacity

of tackling congestion is to upgrade the physical capacity of the existing grid infrastructure. However, due to the inherent spatiotemporal uncertainty of DER, such up-gradation may require a large initial investment of capital and frequent network restructuring funds thereafter. Other congestion handling techniques [7] involve the use of generation rescheduling [8], FACT devices [9] and available transfer capacity (ATC) [10]. The use of power control devices can only relieve network congestion, which is ultimately bounded by the maximum physical capacity of the network. Results from work in [11] provide chronological information proving that DER and market-based congestion methods are more efficient than those incorporating the centralized use of FACT devices. For similar reasons, transformer tap changers (TTC) and phase shifters to mitigate congestion may no longer be viable. Therefore, there is still an inevitable need to develop computationally efficient congestion-mitigating techniques, which are better at handling uncertainties in real-time [12].

1.1. Motivation

The congestion alleviation strategies based on DR programs [13–16] can provide load-supply flexibility to the local grid operators by convincing retail users to modify their energy usage patterns. Prosumers' active management of their DER, complying with operator instructions, can earn them rewards through discounted utility bills [17]. DR methodologies to minimize local voltage-violation of power lines using direct control of the appliances, as developed in [18], can influence consumer convenience negatively. Additionally, due to regulatory policies, it might be unrealistic for the DSO to alter the user loads directly. Instead of DSO altering the load directly, the proposed strategy in this research work brings the aggregator in close coordination with end-users and ensures user willingness through a market-based approach. Aggregators guarantee that user comfort and convenience are not violated while reshaping their consumption patterns and rescheduling the demand to mitigate network congestion and minimize energy consumption costs.

1.2. Literature review and research gaps

Many researchers have deployed market-based mechanisms to implement DR-based methodologies to combat congestion problems. On a shorter time scale, the local grid operators can exploit the market-based DR potential to address the distribution level network congestion [19]. In [20], a probabilistic approach is utilized to reduce the frequency of violating the allowed voltage levels, and the work in [21] described the mechanism of how commercial aggregators can make use of the aggregated load flexibility from individual consumers for congestion mitigation. These works ignored the consideration of forecast errors. A technique termed i-energy is proposed for congestion management in [22]. It utilized potential games between participants to control the loads and deploy other DERs. However, the calculation of incentives is assumed to be based on the predefined loading levels of prosumers. A virtual power plant with photovoltaic (PV) panels and dedicated ESS to address the congestion problem is proposed in [23]. The designed problem is planning rather than mitigating congestion in real-time. The model in our work uses real-time FHL and EV user preferences

Table 1
Summary of various characteristics relating to congestion researched in recent literature.

Ref.	Characteristic						
	Rebound effect	User comfort	Network constraints	Forecast errors	Power imbalance	Main objective	Solution
[29]	✓	x	✓	✓	✓	✓	Offline
[30]	✓	✓	x	x	x	EC and Cong.	Offline
[31]	✓	✓	✓	✓	✓	EC	Offline
[32]	✓	✓	x	x	x	EC	Offline
[33]	✓	✓	x	✓	✓	DP	Offline
[34]	x	✓	x	✓	✓	FLX	RT
[35]	✓	✓	x	x	x	FLX	RT
[36]	x	✓	x	x	x	DP	Offline
[37]	x	✓	x	x	x	LMP	Offline
[38]	x	✓	✓	x	✓	DP	Offline
[39]	x	✓	✓	x	✓	DP	Offline
[40]	x	✓	✓	x	x	DP	Offline
[41]	x	✓	✓	✓	✓	LMP	Offline
[42]	x	x	✓	x	✓	NP	Offline
[43]	x	x	✓	✓	✓	DP	Offline
[44]	x	x	x	x	✓	DP	Offline
[45]	x	✓	✓	✓	✓	EP	RT
[46]	x	✓	✓	✓	✓	EC	RT
[47]	x	x	✓	✓	✓	EC	RT
[48]	✓	x	x	✓	✓	PC	RT
[49]	x	x	✓	✓	✓	RI	RT
[50]	x	x	✓	✓	✓	EC and FLX	RT
[51]	✓	x	✓	✓	✓	OC and RC	Offline
pro	✓	✓	✓	✓	✓	**EC and Cong.**	**Online**

✓: considered **x**: not considered **EP**: Expected Profit **EC**: Energy Cost **PC**: Planning Cost **DP**: Dynamic Pricing **RC**: Reliability Cost **LMC**: Locational Marginal Pricing **NP**: Nodal Prices **RI**: Resilience Indices **FLX**: Flexibility **OC**: Operational Cost **pro**: Proposed **RT**: real-time.

data which lets the aggregators make much more efficient rescheduling decisions than the day-ahead predictions, which always lead to considerable deviation errors.

Congestion management involves different cost-minimization aspects, as shown in Table 1 from various entities involved. The proposed DR methodology in [24] addressed the congestion problem by considering transformer overloading monetary cost, is limited to the transformer overloading penalty cost only, and lacks a smarter scheduling mechanism to enable aggregators to exploit available resource flexibility better. The Stackelberg game distributes incentives among participating entities under a multi-agent scenario in [25]. The model aims at minimizing RES and load curtailment by smartly scheduling the flexible resources through estimated operational points in the day-ahead energy market. In [26], a virtual storage system is modeled to represent the aggregated FHL. Distributed locational marginal prices (LMPs) are calculated iteratively to exploit the prosumer side flexibility. A robust optimization-based approach is used in [27] to model ADN's DR-based congestion management strategy. The authors propose a ledger-based automated congestion management technique in [28], which uses an agent-based hierarchical method. The Majority of these approaches are based on the so-called iteratively optimized pricing algorithms, which ignore end-user convenience constraints. Pricing decisions obtained through such mechanism, mostly day-ahead, apparently seem to relieve the congestion and bring line loadings within acceptable values. However, such models do not define constraints related to individual user tolerances and comfort levels related to load-shifting and curtailment, rendering the obtained solutions impractical. The strategy proposed in this paper, implement the DR program in real-time. Aggregator facilitates DSO in altering the demand profile of participating users subject to the network conditions satisfying EV users' charging preferences.

The proposed method uses a market-based approach. Aggregators do not need any information about the network conditions in advance as it is integrated into the real-time price communicated by the DSO. Most recently, authors in Refs. [45–47] devised frameworks to optimize the market clearing price, system economics improvement, and flexibility pricing strategy, respectively. These works used the unscented transformation method to model uncertainties of load and RES while considering operational constraints such as renewable generators and different ESSs. While this strategy relies only on meeting certain individual constraints to lower the operational costs but does not deploy any framework for congestion alleviation of the network. Unlike these works, we have specifically formulated a detailed EV charging station model under an aggregator to alleviate the network congestion. Robust optimization based on information-gap decision theory was used in [48] to optimize a planning problem to minimize the construction, maintenance, and storage degradation cost. Dissimilar to this work, which is based on a planning problem for the future power infrastructure, our work is focused on leveraging the existing resources to alleviate the congestion problem. Authors in [49] have focused on minimizing the total cost of the smart distribution system operation, which comprises flexible virtual power plants, in case of a natural disaster to enhance the resiliency of the system. The objective of the problems addressed in Refs. [50,51] is to minimize the energy cost and maximize system flexibility. Incentive-based DR is deployed to reward the participating entities and the developed problem is solved using scenario-based stochastic programming. It is well known that scenario-based solutions rely on probabilistic forecasts based on historical data and may not accurately predict future events [5]. Whereas, in this work, we have designed a LO-based strategy to solve the RCM problem in an online fashion that does not rely on unrealistic future predictions.

The procedure described in [52] shows how effectively a data transmission traffic operator can coordinate with the market operator to alleviate feeder-level congestion in ADN. Authors in [53] proposed a combined nodal and uniform pricing algorithm to maintain voltages under allowed levels. It maximizes aggregated social welfare function of participants who use ESS for backup. They use ESS to store energy during the off-peak periods and withdraw in the On-peak hours when the probability of congestion is higher. However, installing ESS exclusively for such purpose may not be economical due to battery fast aging phenomenon [54].

Given current progress in the control, monitoring, information, and communication technology (ICT), EV charging can be treated as an elastic load and may be altered through the electricity price signals in real-time. In view of this, existing congestion management techniques have realized the coordination among the EV users and aggregators in

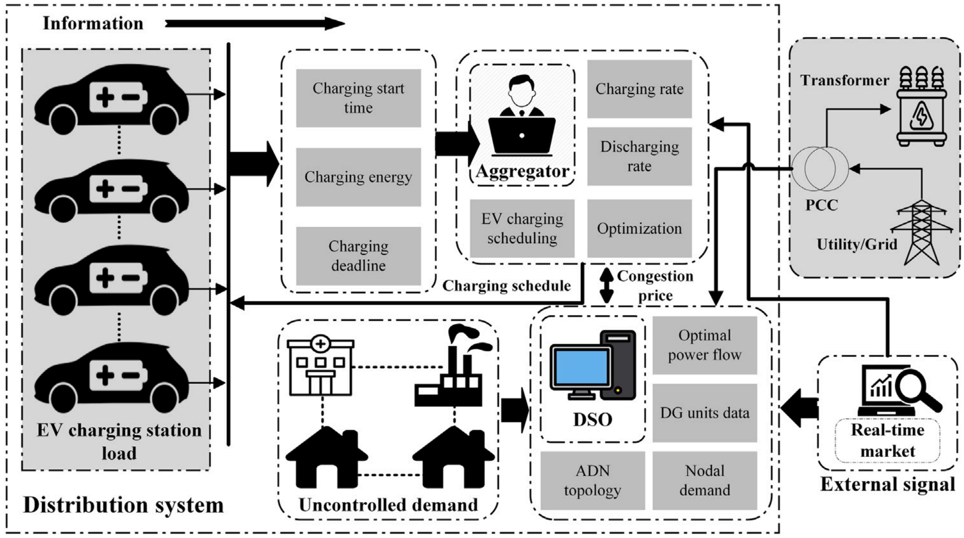

Fig. 1. Schematic diagram for the proposed RCM algorithm.

ways that are supposed to assist grid operation and minimize the charging cost. However, the current approaches have overlooked one aspect of paramount importance, i.e., EV user behavior. Most EV charging control models rely on unrealistic EV availability assumptions [55]; for example, in [56], repercussions of uncoordinated charging of EVs and air pollution are estimated using the DR program and considering RES output variability. RES output is estimated by scenario generation and reduction method. Consequently, such models may compromise user comfort while implementing DR schedules.

1.3. Main contributions

A real-time scheduling algorithm incorporating a DR strategy involving EV and FHL is designed to address the aforementioned issues in the existing congestion alleviation algorithms. Aggregators at different nodes of the ADN collect EV charging preferences data and FHL demand via a data submission mechanism and estimate the load in the next time slot. DSO receives the overall demand from different aggregators and runs DCOPF to estimate the congestion cost in the network. Considering the congestion signal, the real-time electric price, and user preference data, aggregators reschedule the EV and FHL demand using LO to minimize the overall operational cost. The benefits of the proposed real-time congestion management (RCM) scheme are summarized as (1) The developed algorithm is computationally efficient and suitable for real-time practical operations. (2) It does not need information about the probability distribution of EV charging load, FHL, and energy prices. (3) Aggregators only need the information for the current time slot to make the scheduling decisions in real-time. This minimizes forecast errors and makes it suitable for handling uncertainty. The major contributions of this research work are described below:

1. An RCM mechanism based on the LO algorithm is designed. It addresses three main challenges of real-time applications in ADN, i.e., uncertain user behavior, large computational cost, and forecast errors.

2. Unlike the existing approaches, this research considers the different aspects of user convenience in DR and in-depth modeling of EV and FHL scheduling constraints.

3. The performance is compared with other benchmark algorithms, e.g., the greedy algorithm, to prove the efficiency of the proposed strategy.

The rest of the paper is organized as follows. A detailed overview of the proposed RCM scheme, comprising various models, e.g., aggregator and DSO problems, is presented in Section 2. Section 3 describes transformation of the offline model into an online one and then solving it using the LO technique. The performance of the proposed strategy is discussed in Section 4. Finally, Sections 5 and 6 analyze the simulation results and conclude the paper.

2. Distribution-level power network congestion management system overview

An overview of the participating entities and the underlying relations for congestion management is presented in this section. The power for charging EVs and supplying the non-EV loads is drawn from the transmission grid or distributed generators (DGs) inside the ADN. It is inconvenient for small independent consumers to participate directly in the wholesale electric market as it requires a considerable response time and communication infrastructure. Thus, the role of an aggregator as an intermediary entity between DSO and individual small-scale DR participants becomes inevitable. With emerging power electronics and modern ICT, aggregators can develop the necessary infrastructure to aggregate tiny consumers. It can optimize the use of the DER, which may maximize social welfare for the individual participants and contribute towards minimizing grid operational costs and enhancing reliability. The model presented for RCM in this work jointly optimizes EVs and FHL to participate in the DR program. It is assumed that there are long-term DSO-aggregator and aggregator–prosumer bilateral contracts. It is possible that some users might get a congestion price higher than others solely due to being connected to a different position on the network. Consequently, consumers are only liable to pay the energy consumption cost, not the congestion cost. The congestion signal is only meant to help the aggregator to make better rescheduling decisions. However, it is worth emphasizing that EV users should be compensated for participating in the DR and helping DSO relieve the congestion in the ADN. In the proposed aggregator framework, on the one hand, the DR guarantees monetary welfare for the aggregators and rewards for end-users in the form of discounted utility bills. There are several other well-established mechanisms [57] through which this compensation can be allocated, documented, and agreed upon by both the end-users and aggregators in the bilateral contracts. However, developing a detailed model for such a mechanism is not the prime focus of this research work.

A set of aggregators is denoted by $a \in A = \{1, 2, ..\}$ geo-distributed inside the test ADN. Under each aggregator, in a given time slot, we denote the set of EVs as $e \in E_a(t) = \{1, 2, ..\}$. The aggregator's scheduling algorithm controls the charging profile of each EV e.

The schematic diagram for the proposed RCM scheme is shown in Fig. 1. The EV user communicates the charging preferences to the aggregator through an information collection interface as shown on the left side of the schematic diagram. Aggregators receive real-time information on energy prices from the electricity market, depicted on the bottom of the right side of the diagram, and the congestion prices from the DSO interface, as shown in the lower middle part of the diagram. Aggregator plays a vital role in processing the charging information received from EV users and households, as drawn at the center of the diagram. The point of common coupling (PCC) of the ADN to the utility grid is shown at the top right side of the diagram.

The day-ahead clearing of certain resources at specific times in the day-ahead market requires each participant to commit to that resource in real time. However, the real-time dispatch capability of such resources is subject to maintaining network security and ensuring fair play in the energy market, which may not necessarily rely on the exact values of parameters cleared in the day ahead. Therefore, in the proposed work, we do not emphasize the exact business model to calculate compensation/penalty for the participant's load deviation from the committed schedule. Therefore, it is assumed that the aggregators participating in the DR program can declare a self-schedule in real time based on the current market and network status. Interested readers are referred to the work in [58] for further understanding of such business models.

In the forthcoming part of this section, the model constraints associated with the aggregator and DSO optimization problem will be described. An offline problem is formulated to minimize the long-term expected time-average cost. The congestion alleviation mechanism is developed to operate in a time-slotted manner, and each time slot consists of a fixed time duration.

2.1. Overview of aggregator model

The aggregator is assumed to have information about the individual EV users' long-term preferences (EV battery permanent charging characteristics). Aggregators collect real-time charging requests from individual EV users upon their connection via an automated process. The collected charging preference data can be decomposed into the charging start time (connection time-slot), total charging energy required, and the charging deadline. Total charging energy is the difference between the EV state-of-charge (SOC) at the time of the connection and the departure. It can be assumed that the users participating in the DR program have an interface that enables them to submit the charging preferences data in real-time. After collecting charging preferences data, the aggregators schedule the EVs so that the expected time average of charging cost is minimized without violating the EV user's allowed tolerances (e.g., charging deadlines).

2.2. Constraints for EV charging scheduling

It is assumed that the arriving EV users connect EVs for charging according to a stochastic process which follows an unknown probability distribution $\left\{P_{e,a}^{ch}(t)\right\}_{t=1}^{\infty}$. Users connect their EV for charging at the beginning of a time-slot t^{con} (i.e., connection time slot). The EV should be charged by a desired total energy $P_{e,a}^{ch}$ before the disconnection (i.e., departure time-slot) time t^{dep}. The users input the desired charging energy in terms of SOC levels. So, the requested total charging energy can be computed as,

$$P_{e,a}^{ch} = SOC_{e,a}^{dep} - SOC_{e,a}^{con} \tag{1}$$

At the time of EV connection for charging, to ensure the long battery life, assume that the SOC level is confined within the desired bounds due to the manual control of the EV user, i.e.,

$$SOC_{e,a}^{\min} \leqslant SOC_{e,a}^{con} \leqslant SOC_{e,a}^{\max} \tag{2}$$

The above assumption is justifiable as the aggregator has no control over the battery operational limits when EV is out for a trip. It is also obvious that the desired charging energy requested by the user cannot exceed the remaining capacity at the time of connection. Therefore, the amount of desired energy is modified by imposing the following constraint,

$$P_{e,a}^{ch} = \min\left(P_{e,a}^{ch}, SOC_{e,a}^{\max} - SOC_{e,a}^{con}\right) \tag{3}$$

The above constraint ensures that the accepted energy requests always respect the EV's charging capacity limits to avoid fast degradation of battery life. Conversely, from Eqs. (2), (3), it is ensured that after the EV is charged to the requested energy, its SOC cannot exceed the allowed maximum capacity, i.e., $SOC_{e,a}^{dep} \leqslant SOC_{e,a}^{\max}$. Now, let the amount of energy that can be charged in a single time slot be upper bounded as,

$$0 \leq p_{e,a}(t) \leq p_{e,a}^{\max} \tag{4}$$

We do not consider vehicle-to-grid (V2G) functionality in the proposed model, i.e., $p_{e,a}(t) \geq 0$, since it requires sophisticated infrastructure to support the integration of EVs in V2G mode, and it is still not clear whether EV users can benefit by providing such service while overcoming the battery degradation cost [59]. Now assume that the EV starts charging immediately as soon as it is connected for charging with a maximum per-slot energy $p_{e,a}^{\max}$ continuously in every time-slot, then, the minimum time-slots $t^{\min}$ needed to charge the EV by the total desired energy $P_{e,a}^{ch}$ can be computed as $t^{\min} = P_{e,a}^{ch} \big/ p_{e,a}^{\max}$. If the EV were not part of the DR program, it would start charging immediately as soon as it has established a connection with the grid and should complete the charging by spending the minimum number of time slots, i.e.,

$$P_{e,a}^{ch}(t) = \sum_{\tau \in T^{\min}} p_{e,a}^{ch}(\tau) \tag{5}$$

Alternatively, if the EV is scheduled by the aggregator to be charged by an amount of energy $p_{e,a}(t)$ considering the congestion and the spot energy price to minimize the charging cost, and also ensure that the EV is charged to the requested energy $P_{e,a}^{cha}$ level before the deadline t^{dep}, then the charging delay of an EV e, t^{tol} (in several time-slots), the EV user is ready to tolerate can be computed as $t_{e}^{tol} = t^{dep} - t^{con} - t^{\min}$. Conversely, the set of the maximum number of time slots an EV is available for charging can be defined as,

$$T^{ch} = \left\{t^{con}, t^{con}+1, \ldots, t^{con}+t^{\min}, \ldots, t^{dep}\right\} \tag{6}$$

It is now clear from Eqs. (4), (6) that the aggregator shall charge the EV to the requested energy level before the user-defined deadline, i.e.,

$$P_{e,a}^{ch} = \sum_{\tau \in T^{ch}} p_{e,a}(\tau),\ \forall e, a \tag{7}$$

The energy supplied to charge an EV in a time-slot $p_{e,a}(t)$ incurs a cost $p_{e,a}(t)\, u^{en}(t)$. For all the EVs e under an aggregator a, this cost can be computed as,

$$c_{a}^{en}\left(p_{a}^{en}(t), t\right) = \mu^{en}(t)\, p_{a}^{en}(t) \tag{8}$$

where $p_{a}^{en}(t)$ denotes the energy in a single time-slot supplied to all the EVs under an aggregator a, i.e., $e \in E^{a}(t)$, can be computed as,

$$p_{a}^{en}(t) = \sum_{e \in E^{a}(t)} p_{e,a}(t) \tag{9}$$

Similar to the energy cost as computed in Eq. (8), congestion price can be calculated as given below,

$$c_{a}^{cong}(t) = \mu_{b}^{cong} p_{a}^{en}(t) \tag{10}$$

where μ_{a}^{cong} is the monetary price due to congestion. This congestion price is calculated by solving the DCOPF problem by the DSO and communicated to the aggregator as a signal for knowing network conditions to alleviate the congestion inside the ADN. Congestion prices are maybe different for different nodal locations in the ADN. Now let us recall that the per-slot charging requests submitted by the users as defined in Eq. (5) may not be completely fulfilled in a single time slot. Aggregators may optimize the charging process through a scheduling strategy to minimize charging costs. It may shift a portion of requested charging energy to be supplied in the upcoming time slots, anticipating lower energy and congestion prices. To enhance the user charging experience, the delayed charging requests are penalized in the following constraint,

$$c_a^{sh}\left(p_a^{sh}(t), t\right) = \alpha_{sh}\left(p_a^{sh}(t)\right)^2 + \beta_{sh} p_a^{sh}(t), \forall a \tag{11}$$

where α_{sh} and β_{sh} are the coefficients of the shifted charging energy penalty function and $p_a^{sh}(t)$ is the portion of requested charging energy shifted and can be computed using Eqs. (5), (7) as given below,

$$p_a^{sh}(t) = \sum_{e \in E^a(t)} \left(p_{e,a}^{ch}(t) - p_{e,a}(t)\right), \forall e, a \tag{12}$$

The quadratic function for penalty discourages the shifting of a too large a portion of energy requests while seeking a trade-off between charging and user-comfort violation cost.

2.3. Household loads model

Consider FHL registered to participate in DR program under an aggregator a inside ADN. Assuming that the participating households have smart loads, such as heating and cooling appliances. Assume that maximum $L_a^{\max}(t)$ and critical household loads (CHL) $L_a^{crit}(t)$ are generated by the user itself through some intelligent algorithm. The real-time FHL demands are supposed to be non-negative i.i.d stochastic processes. Aggregator's DR policy must satisfy the CHL such that $L_a^{\max}(t) - L_a^{curt}(t) \geqslant L_a^{crit}(t)$. Thereafter the amount of dispatched household demand after curtailment $L_a(t)$ shall meet the following constraint,

$$L_a^{crit}(t) \leqslant L_a(t) \leqslant L_a^{max}(t) \tag{13}$$

where $L_a^{curt}(t) = L_a^{\max}(t) - L_a(t)$ determine the curtailed household demand. To respect the user-comfort, FHL demand curtailment is confined within the allowed limits by introducing the following constraint,

$$\lim_{t \to \infty} \frac{1}{T} \sum_{t=1}^{T} \mathbb{E}\left[\frac{L_a^{curt}(t)}{L_a^{flex}(t)}\right] \leqslant \phi_a \tag{14}$$

where $L_a^{flex}(t) = L_a^{\max}(t) - L_a^{crit}(t)$ and the curtailment ratio $L_{l,a}^{curt}(t) \big/ L_a^{flex}(t)$ represents the percentage of unfulfilled FHL. This constraint makes sure that the curtailed portion of the FHL always remains below a user-specified threshold $\phi_a \in \left[0 \quad 1\right]$, complying with his/her tolerance. A smaller curtailment coefficient value reflects less tolerance towards load shedding and guarantees better power service quality. To avoid very high load supplying costs (alternatively to lower the congestion), a penalty function is introduced to impose a monetary cost of user discomfort as a result of these dropped demands,

$$c_a^{curt}\left(L_a^{curt}(t), t\right) = \alpha_{curt}\left(L_a^{curt}(t)\right)^2 + \beta_{curt} L_a^{curt}(t), \forall a \tag{15}$$

2.4. DSO problem model

A great amount of work reveals that the results obtained through DCOPF are in close agreement with that of the ACOPF. The fast convergence time of DCOPF formulation makes it more suitable for the system operators to prefer it for real-time applications. Recently, DCOPF has been widely adapted to solve various congestion problems, e.g., dynamic tariff-based approach for ADN [29], distributed LMPs for optimal EV charging [60], congestion management with DR considering uncertainties [61], congestion management in ADN through DR [40] and with high penetration of RES in [62]. Therefore, in this work, DCOPF is used to devise distributed LMPs to calculate the prices at different locations for active power consumption. In this model, DSO does not use LMPs data from the day-ahead market or rely on assumptions regarding the probability distribution of controllable and uncontrollable loads. The prices are calculated from the real-time load conditions and only consider the current state of the network. DSO can use the proposed algorithm for RCM without requiring any data from the day-ahead cleared to market and without considering any load forecast. It can avoid the errors in the calculation of congestion pricing stemming from the deviation in LMPs and anticipated load in actual real-time operation. None of the existing literature has incorporated this deviation error in the proposed models for the RCM. Existing literature mostly relies on the information obtained from the day-ahead auction markets and predicted spot prices.

$$\mu_b^{LMP}(t) = \mu^{ene}(t) + \mu_b^{cong}(t) + \mu_b^{loss}(t) \tag{16}$$

Since the DSO considers a lossless DCOPF problem, the energy loss component of the LMP can be neglected, i.e., $\mu_b^{loss}(t) = 0$. The cost incurred to DSO for delivering quality power inside the ADN can be computed as,

$$c^{dso} = \sum_{b \in B} \eta_b(t) p_b^g(t) \tag{17}$$

where, $\eta_b(t)$ is the per-unit energy dispatching price at bus b in time slot t. This price is calculated such that the total demand (without implementing the DR) can be fulfilled through the real-time wholesale spot market. In the events of congestion, the calculated price is based on the assumption that there are distributed generators that can be procured in real-time near congested locations (possibly more expensive than base generators at far locations). Next, the energy balance constraint is given below,

$$\sum_{b \in B} p_b^g(t) = \sum_{b \in B} p_b^d(t) \tag{18}$$

where $p_b^d(t)$ is the nodal demand estimated by the DSO at the beginning of every time slot. It can be computed as follows,

$$p_b^d(t) = p_b^{ch}(t) + L_b^{max}(t) + p_b^{chl}(t) \tag{19}$$

where $p_b^{chl}(t)$ is the total CHL at bus b. Whereas $p_b^{ch}(t)$ are the total per-slot charging requests accepted at the start of the time-slot t at bus b. The total nodal demand $p_b^d(t)$ is a state variable in the DSO problem and is updated and fed back at the beginning of every time slot to recalculate the LMPs. This feedback procedure makes this RCM algorithm dynamic and leaves negligible or no margin for errors compared to the day-ahead static scheduling. The constraint reflecting the limited physical capacity of the transmission facility is described below,

$$\sum_{b \in B} GSF_{k-b}(t)\left(p_b^g(t) - p_b^d(t)\right) \tag{20}$$

where $Limit_k$ is the power capacity of branch k and $GSF_{k-b}(t)$ is the generation shift factor (GSF) of transmission facility b due to a unit shift in generation at bus b. The calculation of GSF is affected by the selection of the slack bus. This study considers the bus connected to the transmission line as the slack bus. The generation capacity limits at a specific location can be represented as,

$$G_b^{\min} \leq p_b^g(t) \leq G_b^{\max} \tag{21}$$

Mathematically, the LMP of a bus is the dual-variable corresponding to the power balance constraint of that bus. The Lagrangian function of the DSO model is formulated as

$$\begin{aligned}\psi(t) = &\left(\sum_{b \in B} \eta_b(t) p_b^g(t)\right) - \omega(t) \cdot \left(\sum_{b \in B} p_b^g(t) - p_b^d(t)\right) \\ &- \sum_{k \in K} \lambda_k(t) \cdot \left(\sum_{b \in B} GSF_{k-b}(t)\left(p_b^g(t) - p_b^d(t)\right)\right) \\ &- Limit_k\end{aligned} \tag{22}$$

where, $\omega(t)$ and $\lambda_k(t)$ are the "Lagrangian Multipliers" of power balance and line power capacity limit constraints. Differentiating the above Lagrangian function gives the LMP as follows.

$$\mu_b^{LMP}(t) = \frac{\partial \psi(t)}{\partial p_b^d(t)} \tag{23}$$

$$\mu_b^{LMP}(t) = \omega(t) + \sum_{k\in K} \lambda_k(t) \cdot GSF_{k-b} \tag{24}$$

where $\omega(t)$ denotes the base energy price. Whereas, $\sum_{k\in K} \lambda_k(t) \cdot GSF_{k-b}$ represent the marginal cost due to the congestion. The congestion component of the total energy consumption costs at a bus b at time t can be calculated as given below

$$\mu_b^{cong}(t) = \sum_{k\in K} \lambda_k(t) \cdot GSF_{k-b} \tag{25}$$

The terms congestion cost and congestion signal are used alternatively in the manuscript. Congestion cost calculated in Eq. (25) can be used as the dynamic signal, carrying real-time network state information to the aggregators. It is not a binary variable meant for YES or No decisions but reflects the severity of congestion on a transmission facility. It plays a critical role in deciding the amount of energy supplied in a time slot along with other costs incorporated in the objective function of the aggregator problem.

2.5. Offline problem for congestion management in ADNs

The overall cost function of the aggregator problem comprises energy consumption cost, the congestion cost, the penalty incurred due to FHL curtailment, and the delay in fulfilling the EV charging requests,

$$\begin{aligned} C_a(t) &= c_a^{en}\left(p_a^{en}(t), t\right) + c_b^{cong}\left(p_a^{en}(t), t\right) \\ &+ c_a^{sh}\left(p_a^{sh}(t), t\right) + c_a^{curt}\left(L_a^{curt}(t), t\right) \end{aligned} \tag{26}$$

where $c_a^{en}(\cdot)$, $c_a^{sh}(\cdot)$, $c_a^{curt}(\cdot)$ are the cost of energy charged to the EVs and FHL, the penalty for shifting EVs charging demands and the penalty cost for the curtailed FHL, respectively. The cost of purchasing energy from the real-time spot market is calculated is given below

$$c_a^{en}\left(p_a^{en}(t), t\right) = \mu^{en}(t)\, p_a^{en}(t) \tag{27}$$

where $p_a^{en}(t)$ is the total energy supplied to EVs and FHL during a time slot and can be determined as given below,

$$p_a^{en}(t) = \sum_{e\in E^a(t)} p_{e,a}(t) + \sum_{l\in L_a} L_a(t), \forall e, a \tag{28}$$

At the start of every time slot, DSO calculates the congestion price by solving the given below DCOPF problem,

$$\begin{aligned} &\min\ c^{dso} = \sum_{b\in B} \eta_b(t)\, p_b^g(t) \\ &\quad sub\ to:\ (17)–(25), \forall t \end{aligned} \tag{29}$$

The network condition is estimated by solving the DSO problem described in Eq. (29). It is sent to the aggregators as an additional price signal on top of the energy price information received from the energy spot market. This congestion price $\mu_b^{cong}(t)$ is defined by Eq. (25) in Section 2.4. Based on these price signals and user-defined preferences and deadlines described in Sections 2.2 and 2.3, aggregators optimize scheduling decisions. Now, the various state variables for the aggregator's cost minimization problem can be represented as a concatenated vector

$$s(t) = \left\{p_a(t)\ ,\ \mu_a(t)\ , t_{e,a}(t)\right\} \tag{30}$$

where $p_a(t) = \left\{p_{e,a}^{ch}(t), L_a^{\max}(t), L_a^{crit}(t)\right\}$ is the upper bound and CHL, and per-slot EVs charging requests submitted to the aggregators at the start of each time-slot, $\mu_a(t) = \left\{\mu_a^{cong}(t), \mu^{ene}(t)\right\}$ is the vector of energy and congestion prices at different nodes of the ADN and $t_{e,a}(t) = \left\{t^{con}(t), t^{dep}(t)\right\}$ is the vector of EVs connection (arrival) and disconnection (departure) time. The concatenated vector of the aggregator problem's decision variables is formulated as given below,

$$d_a(t) = \left\{p_{e,a}(t), L_a(t), p_{e,a}^{sh}(t), L_a^{curt}(t)\right\} \tag{31}$$

Finally, the infinite time horizon expected time average cost minimization problem is designed as given below,

$$\begin{aligned} P1:\ &\min_{\{\bar{C}_a(t)\}} \lim_{T\to\infty} \frac{1}{T} \sum_{t=0}^{T-1} \mathbb{E}\left\{C_a(t)\right\} \\ &sub\ to:\ (1)–(12),\ (13)–(14),\ (29), \forall t \end{aligned} \tag{32}$$

Problem P1 is stochastic, mainly because of the random EV arrival process, time-varying FHL, volatile spot, and congestion prices. Finding the optimal solution to such problems is very challenging. Moreover, decision variables of P1, such as FHL curtailment ratio and heterogeneous EV charging completion deadlines, are coupled across time. In Section 3, instead of optimizing the aggregator's static cost over the infinite time horizon, the time average of the aggregator's overall cost can be minimized slot-by-slot greedily. It can be accomplished via an online strategy incorporating the LO technique.

3. RCM algorithm using Lyapunov optimization

It can be noticed from the problem P1 developed in Section 2.5 that it minimizes the long-term cost of the aggregator. The problem P1 can be solved using any offline algorithm. However, the challenge here is solving it in real-time, which may only use the information about the system states available for the current time slot. The inspiration is designing an algorithm that can operate online and decide the EV charging energy in real-time without requiring any historical information or probability distributions of the uncertainties involved. Optimization techniques based on the Lyapunov framework can be applied after transforming the long-term offline problem into per-slot independent sub-problems. These sub-problems can be solved greedily by incorporating virtual queues and the drift-plus-penalty function. The EV charging scheduling and dispatch of the FHL decisions in the aggregator's problem are based on the novel queuing theory. More specifically, the aggregator creates a queue for EVs with similar charging preferences (e.g., a group with the same delay tolerances regarding the number of time slots) to store the per-slot charging requests. The requests are cleared from the queues, so EVs are charged to the requested SOC level before the user-specified deadline. The EV arrival process and FHL demand requests are assumed to be independent, and the aggregator has no information about its probability distribution. For such a practical scenario, the LO framework, which utilizes queuing theory, can fulfill EV charging demands and dispatch FHL at a minimal cost. It decides the amount of charging energy in each time slot by looking at the energy spot price and dynamic congestion price signal sent by DSO constrained by charging deadlines. Before applying the LO to solve problem P1 in real-time, it must be transformed into a compatible form. The complete procedure for offline-to-online problem transformation is illustrated in Fig. 2.

3.1. Congestion management in real-time

Recently, the LO framework has been used to solve energy management problems in diverse areas, such as energy trading in microgrids [63], real-time ESS sharing [64], online energy sharing among nano-grids [65], data centers cost minimization with storage [66], real-time energy management strategy for a smart-community [67], and online energy flow control of regional integrated energy systems [68]. This work is perhaps the first to develop an application of the LO framework for solving a RCM problem. The solution of the developed offline problem P1 in an online fashion is challenging compared to other existing applications of LO. The complexity of the overall optimization problem is significant due to various constraints relating to arbitrary charging requests. The charging accomplishment and FHL fulfillment decisions while maintaining user comfort simultaneously are inevitably coupled across the time horizon.

A flow diagram in Fig. 3 illustrates the step-by-step mechanism of the designed RCM algorithm. The DSO utilizes network information,

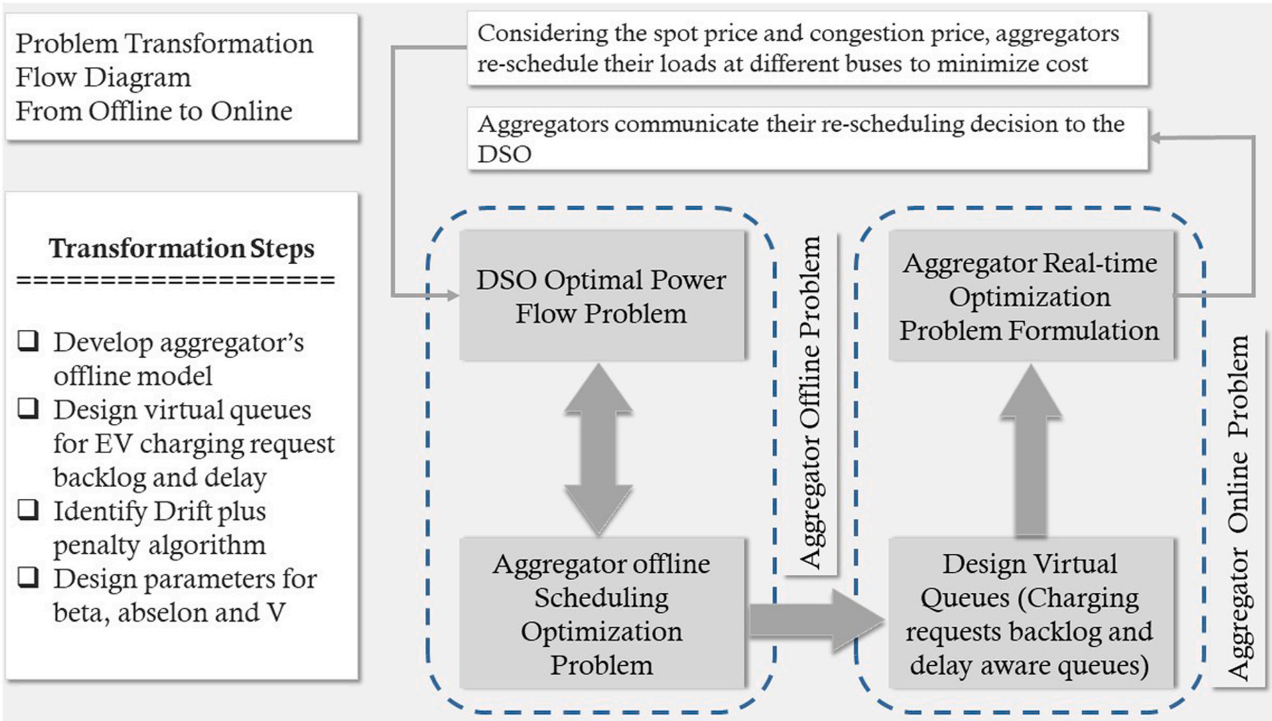

Fig. 2. Offline-to-online problem transformation illustrative diagram.

including the topology of the ADN, line-loading limits, and internal DG limits, as shown on the left side of the diagram. Additionally, the DSO has access to other parameters such as aggregated uncontrollable and flexible nodal demands. By solving an optimization problem based on this information using DCOPF the DSO determines congestion signal. Whereas, the aggregator optimizes the energy scheduling problem by using information stored in the queue backlogs. This information includes EV charging energy requests, household loads, and delay-aware virtual queues. The Aggregators schedule the charging of EVs and manage household loads based on the information stored in virtual queues, congestion signals communicated by DSO, and energy spot prices. Finally, aggregators communicate the energy consumption decisions to the individual EV and household users.

3.2. Virtual queues design

In this subsection, we design virtual queues to handle real-time per-slot EV charging requests as defined in Eq. (5), delay-aware virtual queues to supply EV charging requests before the user-defined deadlines as described in Eqs. (6), (7) and virtual queues to maintain power quality for FHL as described in Eq. (14).

3.2.1. EV charging request queues

The EV charging requests corresponding to different delays are stored in separate queues. The per-slot EV charging requests, as defined in Eq. (5), belonging to similar delays, are stored in a single queue and processed as given below,

$$R_{d,a}(t+1) = \max\left[R_{d,a}(t) - O_{d,a}(t), 0\right] + I_{d,a}(t) \tag{33}$$

where $I_{d,a}(t)$ and $O_{d,a}(t)$ represent the incoming charging requests of EVs belonging to a queue associated with a delay (in several time-slots) $d \in D_a = \{1, 2, ..\}$ at the beginning of a time-slot, whereas, $O_{d,a}(t)$ are the served to charge requests an outgoing portion of the requested charging energy $I_{d,a}(t)$ which is served in time-slot "t". It is obvious from the queue described in Eq. (33) that rather than fulfilling the incoming EV charging requests immediately once received, the service decisions are based on various factors such as the tolerable delay to which the queue is associated with, energy and congestion price signals, etc. What fraction of the requested demand can be fulfilled in the time slot "t" depends on the real-time energy and congestion prices. Generally, if the combined energy and dynamic prices are high, the charging portion the algorithm decides is small; if they are low, the charging portion is relatively large. One more factor contributes while making charging decisions, i.e., how far is the deadline (queue backlog).

From the queues structure described in Eq. (33), the queue backlog may drop below empty, which has no physical meaning. To avoid this situation, the given below constraint is imposed,

$$0 \leqslant O_{d,a}(t) \leqslant \min\left[O_{d,a}^{\max}(t),\ R_{d,a}(t)\right] \tag{34}$$

where $O_{d,a}^{\max}(t)$ is the upper bound of the stored charging requests of EVs which still not-served, i.e., $O_{d,a}^{\max}(t) \leqslant \sum_{e \in E^{d,a}(t)} p_{e,a}^{\max}(t)$ Now let us recall that the service requests for EV charging energy demands $O_{d,a}(t)$ from Eq. (33), is the to-be fulfilled sum of the per-slot disaggregated charging energy demands. However, it is impractical for EV users to request charging energy at the beginning of every time slot. Alternatively, aggregators receive EV charging requests for total energy and use an automated approach to allocate it across multiple slots based on the EV charger characteristics and user-defined preferences. The disaggregation process of the requested charging energy by each EV upon its connection to the ADN was described in Section 2.2.

3.2.2. Delay aware virtual queues for EV charging request fulfillment

A delay-responsive virtual queue is introduced to meet the constraint described in Eq. (7). The Delay responsive virtual queue is designed such that the submitted charging requests are fulfilled before the user-predefined deadline,

$$\begin{aligned} &Z_{d,a}(t+1) = \max\left[\left(Z_{d,a}(t) - O_{d,a}(t) + \varepsilon_{d,a}\right),\ 0\right] \\ &\varepsilon_{d,a} = \begin{cases} +ve, & R_{d,a}(t) > 0 \\ 0, & R_{d,a}(t) \leq 0 \end{cases} \end{aligned} \tag{35}$$

where $\varepsilon_{d,a}$ is a fixed parameter assigned a finite positive value if there are some unfulfilled charging demands. The parameter $\varepsilon_{d,a}$ is designed

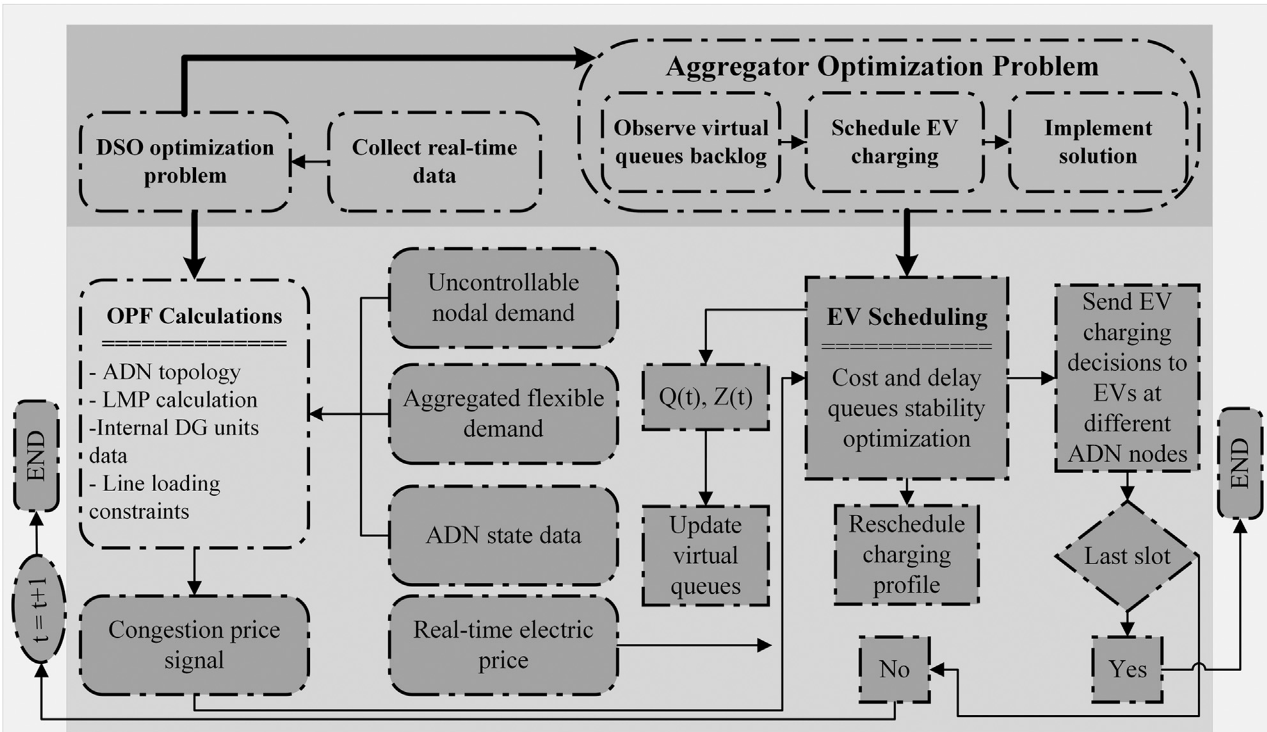

Fig. 3. Flow diagram demonstrating complete step-by-step mechanism of the designed RCM algorithm.

such that when it is tuned to a value, it will push the queues to be stabilized at a rate that will ensure the fulfillment of EV charging request binding to the deadlines associated with the queues. The maximum queuing delay is upper bounded by $\left(Z_{d,a}^{\max} + R_{d,a}^{\max}\right)/\varepsilon_{d,a}$, as shown in the following lemma

Lemma 1. *Maximum Queuing Delay: Assume that the system can be controlled such that $Z_{d,a} \leqslant Z_{d,a}^{\max}$ and $R_{d,a} \leqslant R_{d,a}^{\max}$ for all queues associated with a delay. Then all EV charging requests stored in queues $R_{d,a}(t)$ can be fulfilled with a maximum delay of $\left(Z_{d,a}^{\max} + R_{d,a}^{\max}\right)/\varepsilon_{d,a}$*

Proof. see Appendix A

3.2.3. Virtual queue to ensure quality of power for FHL

A virtual queue is introduced to meet the constraint described in Eq. (14), accomplishing the quality of power (QoP) for FHL demand. The virtual queue starts such that $M_a(0) = 0$ and evolves as given below,

$$M_a(t+1) = \max\left[M_a(t) - \phi_a, 0\right] + \frac{L_a^{curt}(t)}{L_a^{flex}(t)} \tag{36}$$

From queue defined in Eq. (36), it can be noticed that $\phi_{l,a}$ is the FHL fulfillment rate and $L_a^{flex}(t)/L_a^{curt}(t)$ $L_a^{flex}(t)L_a^{curt}(t)$ is the actual serving rate. FHL having identical QoP coefficient values are grouped into a single queue. To ensure the mean-rate-stability of the queue $M_a(t)$, the request and service rates must be equal, i,e., $\lim_{t\to\infty}\frac{1}{t}\mathbb{E}\left[M_a(t)\right] = 0$. This can be proved using the *mean-rate-stability theorem* [69]; however, we omit the proof here for brevity.

To this end, the problem P1 described in Section 2.5 can be modified to express it in terms of time average expected cost, provided the virtual queues designed in the above section are stabilized, i.e.,

$$P2: \min_{\{d_a(t)\}} \lim_{T\to\infty} \frac{1}{T} \sum_{t=0}^{T-1} \mathbb{E}\left\{C_a(t)\right\} \tag{37}$$
$$sub\ to: (1)\text{–}(6), (8)\text{–}(12), (13), (29)\text{–}(36), \forall t$$

Note that in P2, the constraints (7) and (14) from P1 has been replaced with virtual queues in Eqs. (33)–(36). Assuming that the optimal solution to problem P2 is feasible for the offline problem in P1, it can be proved that it is also an optimal solution to problem P1.

3.3. Min-drift-plus-penalty algorithm

The P2 problem in Eq. (37) is still difficult to solve in its current form mainly because of the objective function involving infinite time-average of the cost being minimized and queue stabilization constraints described in Eq. (33)–(14). We utilize the LO framework involving a min-drift-plus-penalty algorithm to address the above-mentioned challenges. Let $\Theta(t) = \left\{R_{d,a}(t), Z_{d,a}(t), M_a(t)\right\}$ denote the virtual queues in the form of a concatenated vector. Then, in each time slot, to quantify the backlog congestion within virtual queues, a Lyapunov function is introduced as given below

$$L(\Theta(t)) = \frac{1}{2}\begin{bmatrix} \zeta \sum_{d\in D_a} R_{d,a}(t)^2 + \gamma \sum_{d\in D_a} Z_{d,a}(t)^2 \\ +\xi \sum M_a(t)^2 \end{bmatrix} \tag{38}$$

where ζ, γ *and* ξ, are trade-off coefficients used to treat the virtual queues independently.

Next, the conditional per-slot drift is described as

$$\Delta(\Theta(t)) = \mathbb{E}\left[\, L(\Theta(t+1)) - L(\Theta(t)) | \,\Theta(t)\right] \tag{39}$$

The min-plus-drift formulation is a method to evaluate the virtual queue expected length evolution given the present-slot state $\Theta(t)$. Explicitly minimizing the drift only may yield stabilized queues at most; nevertheless, it can still cause a huge penalty cost. On that account, the trick is to simultaneously minimize the drift, and penalty term via a function termed as min-drift-plus-penalty expression, i.e., $\Delta(\Theta(t)) + V\left[C(t)|\,\Theta(t)\right]$. Where V, always being a positive constant, provide a trade-off scheme between the demand procurement cost and the penalty cost due to a delay.

Lemma 2. *Lyapunov Min-drift-plus-penalty Algorithm: Subject to the all candidate control policies $d_a(t)$ along all time-slots, the Lyapunov Min-drift-plus-penalty term is upper bounded as*

$$\begin{aligned}&\Delta(\Theta(t)) + V\mathbb{E}[C(t)|\Theta(t)] \leqslant B \\ &+\zeta \sum_{d\in D_a} R_{d,a}(t)\mathbb{E}\left[I_{d,a}(t) - O_{d,a}(t)\middle|\Theta(t)\right] \\ &+\gamma \sum_{d\in D_a} Z_{d,a}(t)\mathbb{E}\left[\varepsilon_{d,a} - O_{d,a}(t)\middle|\Theta(t)\right] \\ &+\xi \sum M_a(t)\mathbb{E}\left[\frac{L_a^{curt}(t)}{L_a^{flex}(t)} - \phi_a\middle|\Theta(t)\right] \\ &+V\mathbb{E}[C(t)|\Theta(t)]\end{aligned} \tag{40}$$

whereas B is a constant term, described as given below

$$\begin{aligned}B = &\sum_{d\in D_a}\left\{\begin{matrix}\left(I_{d,a}^{\max}\right)^2 + \left(O_{d,a}^{\max}\right)^2 \\ +\max\left[\left(\varepsilon_{d,a}\right)^2, \left(O_{d,a}^{\max}\right)^2\right]\end{matrix}\right\}\Big/2 \\ &+\left(1+{\phi_a}^2\right)/2\end{aligned} \tag{41}$$

Proof. see Appendix B

Instead of solving the min-drift-plus-penalty problem directly, the right-hand-side (RHS) of the above-described expression can be evaluated slot-wise in a greedy fashion incorporating the minimization of conditional expectation through an opportunistic mechanism.

3.4. Solving congestion alleviation problem in an online fashion

Considering state vector $s(t) = \{p_a(t) \quad \mu_a(t)\; t_{e,a}(t)\}$ of uncertain inputs parameters, there exist an arbitrary stationary optimization policy influenced by their current values only. It dictate the decision vector $d_a(t) = \left\{p_{e,a}(t), L_a(t), p_{e,a}^{sh}(t), L_a^{curt}(t)\right\}$ and result in a cost that is *(B/V)* far from the optimal. The such developed algorithm is summarized as follows; At the beginning of each time-slot t, the system state vector, as described in Eq. (30), is observed. The per-slot EV charging and FHL demand are communicated to DSO by the aggregator. The congestion price signal is determined by solving the DCOPF problem as described in problem (29). The network state information integrated into the congestion price is sent to the aggregator. The virtual queues backlog $\Theta(t)$ are estimated afterward. Finally, the control decision vector, as defined in Eq. (31) is determined by solving the following online problem P3,

$$\begin{aligned}P3:\ &\min_{\{d(t)\}} VC(t) + \zeta\sum_{d\in D_a} R_{d,a}(t)O_{d,a}(t) \\ &-\gamma\sum_{d\in D_a} Z_{d,a}(t)O_{d,a}(t) - \xi M_a(t)\frac{L_a(t)}{L_a^{flex}(t)} \\ &sub\ to:\quad virtual\ queues\ stabilization, \forall t, a\end{aligned} \tag{42}$$

It is evident that problem P3 does not contain terms that depend on any presumed future or historical distributions. The queue backlogs $\Theta(t)$ are sufficient to consider for control decisions in the next time slot. This property of the Lyapunov formulation makes it a good choice for solving real-time problems of great complexity with notable accuracy and negligibly time compared to other online approaches.

4. Performance analysis

Let the optimal long-term average cost and the cost incurred from the LO be denoted as C^*e and $C^\bullet$, respectively. The optimal cost C^* can be achieved by optimally solving the problem P3 through any possible random control policy, i.e., $d_a^*(t) = \left\{p_{e,a}^*(t), p_{l,a}^*(t), p_{e,a}^{sh*}(t), p_{l,a}^{curt*}(t)\right\}$. Conversely, the same problem P3 can be solved in real-time through the application of min-drift-plus-penalty algorithm as described in Lemma 2, by greedily minimizing the cost in every time-slot, independently, through a control policy, let us call it $d_a^\bullet(t) = \left\{p_{e,a}^\bullet(t), p_{l,a}^\bullet(t), p_{e,a}^{sh\bullet}(t), p_{l,a}^{curt\bullet}(t)\right\}$. Now, the optimality gap between the solution obtained using any other optimal control algorithm, and the LO framework can be characterized through the LO theory as stated in the following theorem;

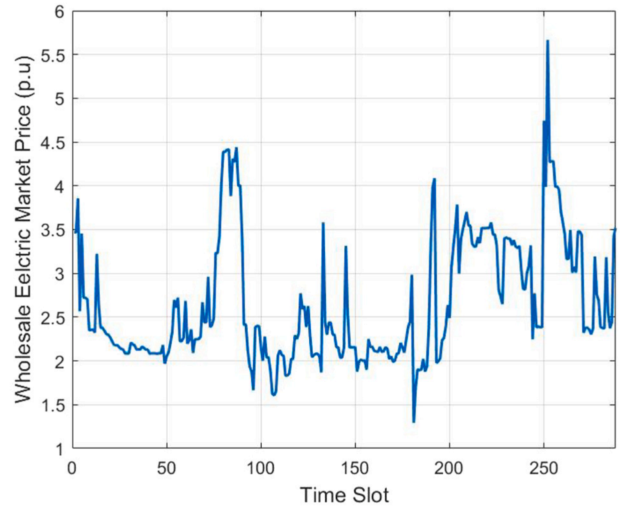

Fig. 4. Real-time wholesale market electric price.

Theorem 1. *The time-average of the total cost C incurred to an aggregator via solving the online problem P3 by participating in DR program is upper bounded by,*

$$\lim_{t\to\infty}\frac{1}{T}\sum_{t=1}^{T}\mathbb{E}[C(t)] \leqslant C^* + B/V$$

where C^* denotes the optimal cost.

Proof. see Appendix C

Theorem 1 proves that the Lyapunov algorithm guarantees the performance bound $C^* \leqslant C \leqslant C^\bullet + B/V$. Whereas the control parameters V and B are discussed in Section 3. The real-time solution obtained through the control policy implemented using LO, i.e., $d_a^\bullet(t) = \left\{p_{e,a}^\bullet(t), p_{l,a}^\bullet(t), p_{e,a}^{sh\bullet}(t), p_{l,a}^{curt\bullet}(t)\right\}$, may not be feasible to the problem P2. Because the choice of parameter V that is greater than the actual may lead to a smaller optimality gap but at the expense of an increase in the average virtual queue backlogs. Large average queue backlogs may alternatively disregard the corresponding constraints, rendering the obtained solution infeasible. Concisely, the value of V provides a trade-off between the cost and queue backlogs' average size. Nonetheless, the careful configuration of constant B and suitable parameter V can guarantee feasible results.

The delay-aware virtual queues ensure that the requested EV charging energy demands $I_{d,a}(t)$ are served before the maximum allowed delay tolerances, i.e., $d \in D_a = \{1, 2, ..\}$

Lemma 3. *Virtual Queues Characteristics: a. The queues $R_{d,a}(t)$ and $Z_{d,a}(t)$ can be characterized as $R_{d,a}^{\max} = V\mu_a^{\max} + I_{d,a}^{\max}$ and $Z_{d,a}^{\max} = V\mu_a^{\max} + \varepsilon_{d,a}$, b. $\varepsilon_{d,a} = \left(2V\mu_a^{\max} + I_{d,a}^{\max}\right) / \left(D_{d,a}^{\max} - 1\right)$*

Proof. See Appendix D

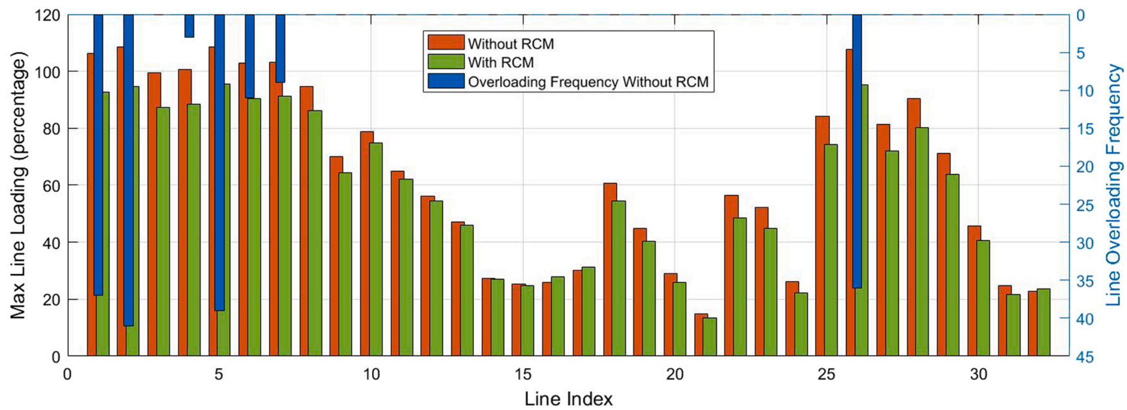

Fig. 5. Line-loading (Line-13) in terms of percentage of line-limit and overloading frequency.

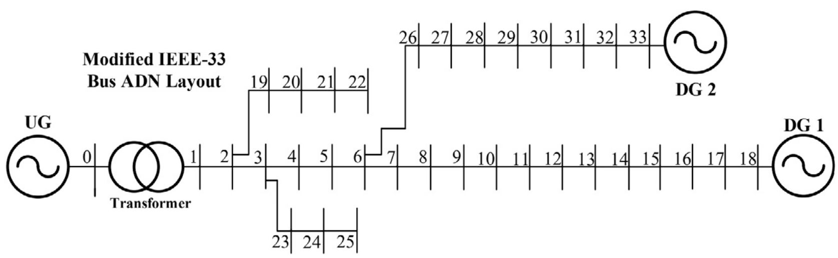

Fig. 6. Modified IEEE 33-bus test ADN layout.

5. Case studies

This section analyzes extensive case study results to demonstrate the performance of the proposed RCM algorithm. First of all, various parameters corresponding to the input data are described. Next, line-loading levels are discussed, such as overloading frequency and percentage of maximum loading limits. The shifted load, charging, FHL request fulfillment delay, and computational cost are presented. At the end of the section, EV charging cost due to the proposed RCM algorithm is compared with the benchmark algorithms.

5.1. Simulation setup

To validate the potential of the proposed algorithm, a modified version of the IEEE 33-bus distribution test network, as shown in Fig. 6, is used. The test ADN comprises 32 load buses, 2 DG buses, and 32 branches. For clarity, in this paper, it is assumed that an aggregator is serving all the loads in the test ADN. However, the results can be easily extended to multiple aggregator cases without affecting performance.

The penetration of FHL demand and EVs are shown in Figs. 8 and 11, respectively. To simplify the analysis, all households and EVs at a bus are aggregated into single but separate residential and EV loads. The CHL demand follows the normal distribution from $[60\%, 90\%]$ of the total household demand. The aggregated household demand follows the typical daily load curve, and individual household loads are obtained from Ref. [70]. The demand curve peaks due to EVs charging mostly coinciding with that of the residential demand [71]; hence, the EV charging demand curve is assumed homogeneous to the residential load curve. Different probability distributions of residential and EV loads may not affect results as the developed real-time model does not rely on any forecast a priori. The battery capacity, maximum SOC, minimum SOC, minimum SOC of connecting EV, and max requested charging energy are set to 100 kWh, 90% of capacity, 10% of capacity, same as minimum SOC and $[50\%, 90\%]$, respectively. The duration of the single time slot is considered 5 min, and the maximum EV charging rate in a time slot is assumed to be 3.33 kWh. Real-time wholesale electric market price data is obtained from Ref. [72] and is shown in Fig. 4.

The proposed algorithm is programmed and solved using CVX, a MATLAB-based software package for disciplined convex programming [73]. The simulation results discussed in this paper are obtained using Intel(R) Core(TM) i5-8265U CPU 1.60 GHz with 8 GB RAM. The per-slot computational cost is shown in Fig. 9. On average, the proposed LO-based algorithm takes 0.55 s to solve the developed online problem, making it suitable for practical applications.

5.2. Simulation results

To analyze the superiority of the LO-based RCM approach, the line-loading at Line-5 with and without the proposed RCM algorithm is demonstrated in Fig. 10. Most of the approaches in the existing literature [74] solely rely on the day-ahead predicted demand at each node of the ADN to estimate the congestion. The performance of such techniques may significantly deteriorate in practical applications as they do not consider forecast errors. Algorithms proposed in this paper do not rely on day-ahead forecasts and use nodal demands at the start of every time slot and communicate to DSO, who calculate the dynamic congestion price in real-time. The computed congestion price is returned to the aggregator to reschedule the loads. To determine the line loading levels shown in Fig. 10, the DSO's DCOPF problem in Eq. (29) is solved twice; (Case-1). Without rescheduled demand and line limits (Case-2). With rescheduled demand and without line limits.

Loading at Line-5 is contributed by demands at nodes 6–18 and 26–33. It can be deduced from Fig. 10 that the loading at Line-5 has reduced significantly due to the rescheduling of loads at nodes 6–18 and 26–33 after considering the dynamic congestion price signal, which is shown in Fig. 7. It is also evident by looking at Figs. 7 and 10 that the proposed algorithm can wisely reduce the line loading during the time slots 210–230 when there is congestion in the network.

Furthermore, in Fig. 5, the efficacy of the proposed RCM algorithm can be demonstrated from another perspective, i.e., it can significantly

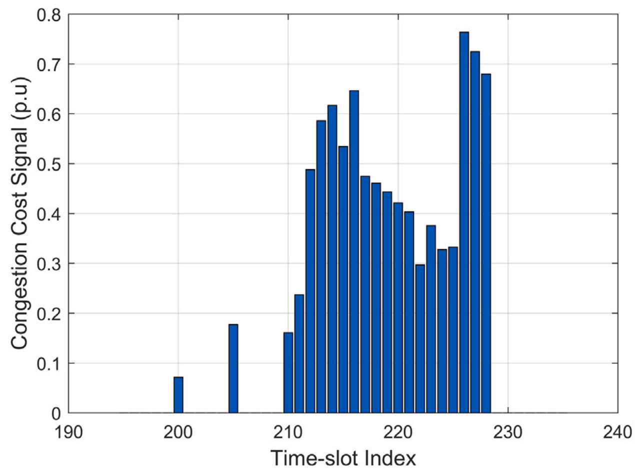

Fig. 7. Real-time congestion price during different time-slots for aggregator located at node-13.

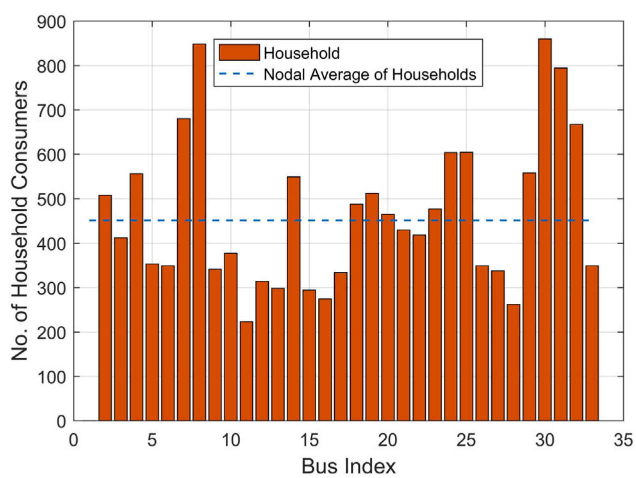

Fig. 8. Distribution of FHL at different nodes of the test network.

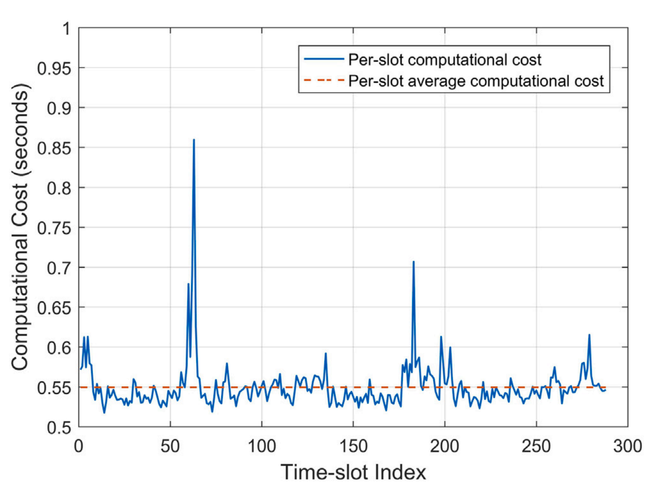

Fig. 9. Per-slot computational cost using RCM algorithm.

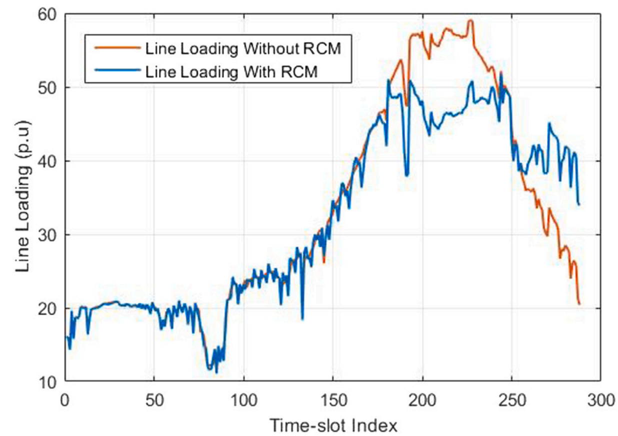

Fig. 10. Line-loadings (Line-27) with and without proposed RCM algorithm.

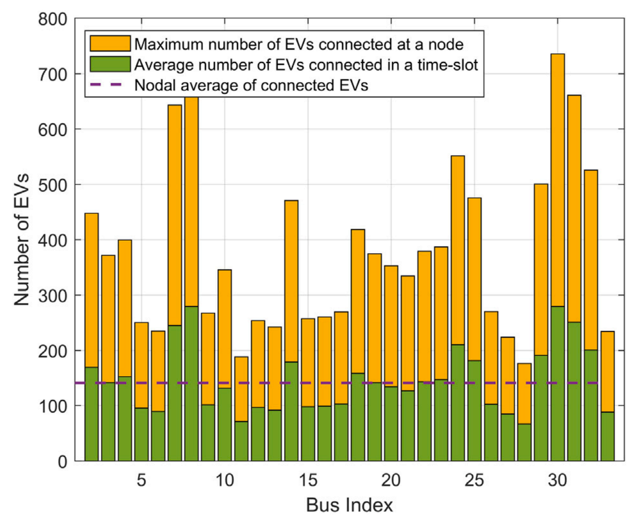

Fig. 11. EV load concentration at different nodes of the test network.

reduce the loading percentage leading to a longer transformer lifetime in the distribution feeders.

From Fig. 13, it can be observed that the RCM algorithm is sensitive in responding to the real-time wholesale electric price and dynamic CCS. Sharp spikes in the shifted-load curve at the circled time slots are due to either high electric prices or high congestion costs. It is clearly able to shift the FHL and EV demand away from peak-hour time slots to avoid congestion. Alternatively, the aggregator can intelligently respond to network conditions communicated by DSO in the form of CCS, which can reduce the line-loading in peak-demand hours.

The time-accumulated average cost incurred for supplying FHL and EV charging demand is compared with the benchmark algorithms, i.e., offline, T-slot look-ahead greedy and without any DR strategy, in Fig. 14.

In the offline algorithm, the underlying uncertain input parameters, such as EV arrival times and congestion price, are all known beforehand. Results obtained by solving the problem using such a deterministic offline approach can help estimate the lower bound of the cost to the problem being solved in real-time. Nevertheless, the results from such offline strategy are nowhere near feasible in practical scenarios where stochasticity of the various input parameters is inherent [75]. Whereas a T-slot look-ahead greedy algorithm uses the values of the input data that are known T-slots in advance, here in this paper, $T = 24$.

From Fig. 14, it can be seen that there is no significant difference until the 100th time-slot between the costs incurred by different strategies other than offline because the variations in different costs related

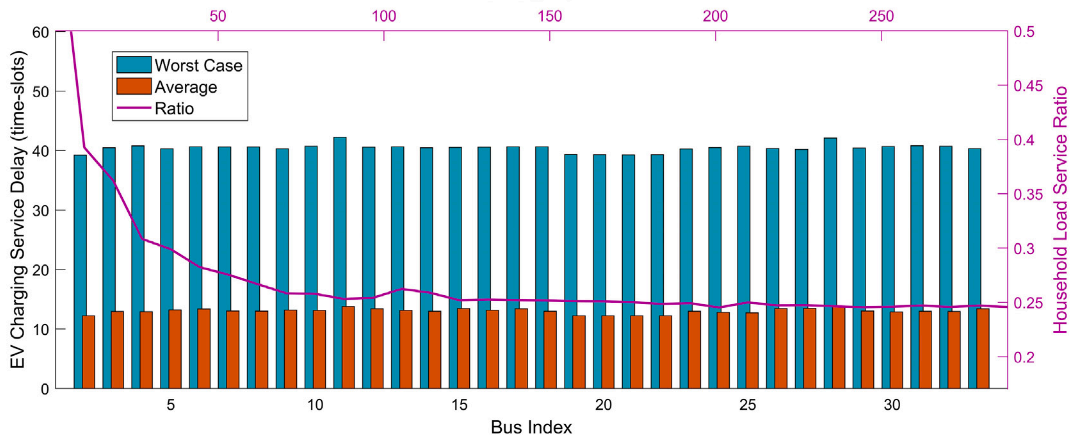

Fig. 12. EV-charging requests service delay and FHL fulfillment ratio.

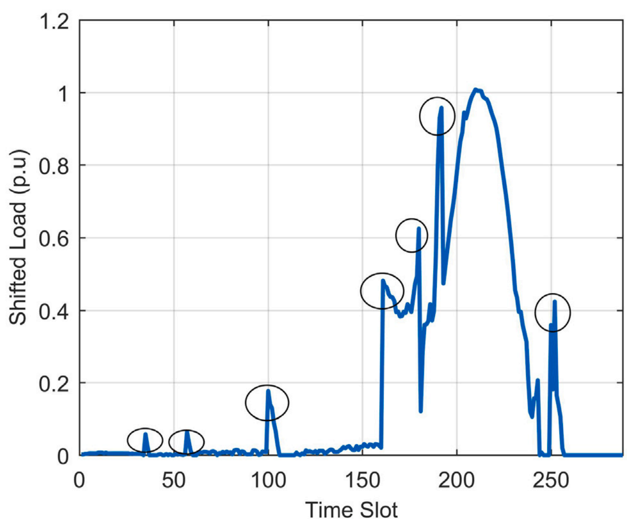

Fig. 13. Shifted load at node-5 in response to varying energy cost and network conditions.

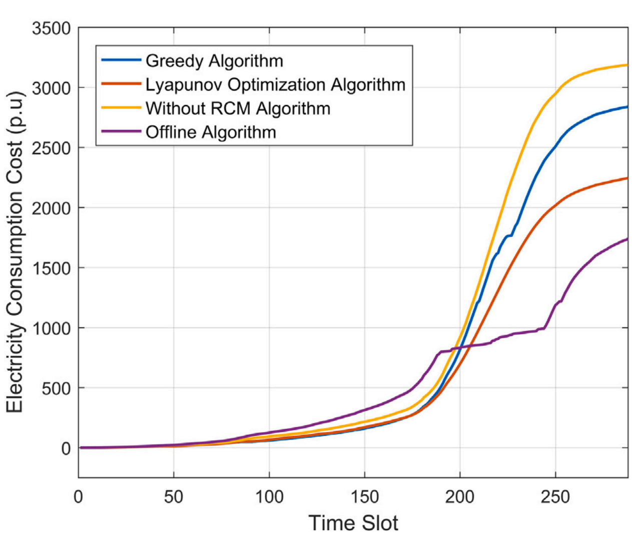

Fig. 14. Time-accumulated cost comparison with benchmark algorithms.

to energy consumption are minimal during the off-peak hours. On the other hand, the offline algorithm incurred more cost until before the 200th time-slot, and there onward, it outperformed other algorithms because of high real-time electric price and high congestion cost during that period. It can do so because it knows the future statistical distributions of the uncertain variables. The highest cost is incurred by the approach which uses no DR strategy. Overall, the performance of our proposed algorithm is only next to that of the offline algorithm.

The delay in fulfilling the energy requests for EV charging and FHL fulfillment ratio is shown in Fig. 12. It can be observed that the worst-case and average delay in completion of the EV charging request on all the buses is in accordance with the preset limits. The time average of the FHL curtailment ratio is higher at the start of the time horizon but quickly converges towards the set limit, i.e., 0.25. The Lyapunov technique's inherent property provides the mechanism to design a resource scheduling strategy such that its convergence utilize the time averages exponentially.

6. Conclusion

A congestion alleviation strategy based on the DR program is proposed in this work. The traditional power networks may increasingly face network overloading conditions due to the increasing share of RES and brisk electrification of the transport sector. Current approaches tackling congestion use direct control ignoring user behavior constraints. Others are largely deterministic and rely on unrealistic assumptions about the probability distribution of the involved random variables. The DR program implemented in this paper incorporates EV charging and FHL, aggregator, and DSO in real-time under a smart distribution scenario.

The developed algorithm incorporates the LO framework and uses a market-based approach instead of direct control. It is designed such that the aggregator does not explicitly rely on DSO for sharing the network conditions. Instead, the dynamic congestion signal carries complete network information required by the aggregator. First, a virtual queue-based procedure is designed to transform the offline congestion management problem into a form that can be solved online. Second, the LO technique is applied to solve the online problem in a slot-wise greedy fashion. It does not require any future probability distribution of the uncertain variables involved in the model. The efficacy of the proposed algorithm is verified through extensive simulations based on the modified IEEE-13 bus test network. The obtained results reveal that the line loadings have notably dropped, and the occurrence of the line over-loading frequency violations are far less than that without the proposed algorithm. It proves that the developed strategy is robust to uncertainties related to EV user behavior and volatile electric prices. The time average of the FHL curtailment ratio and EV-charging requests service delay converges towards the assumed user-set limits, i.e., 0.25 and 10 times-lots respectively. The comparative analysis of cost minimization with other algorithms, such as the greedy algorithm, shows that the proposed algorithm is able to outperform other benchmark algorithms. The limits of the proposed work are that the proposed strategy may not be able to accommodate an EV user to amend its charging preferences in case of an unusual or emergency situation. The proposed algorithm does not consider any probability distributions of user behavior or electricity prices. Therefore, it can be extended to include realistic probability distributions which may further enhance the efficiency of the proposed strategy in certain circumstances.

CRediT authorship contribution statement

Mohan Menghwar: Writing – review & editing, Writing – original draft, Visualization, Software, Methodology, Investigation, Formal analysis, Conceptualization. **Jie Yan:** Validation, Supervision, Resources, Formal analysis. **Yongning Chi:** Validation, Investigation. **M. Asim Amin:** Visualization, Formal analysis. **Yongqian Liu:** Supervision, Resources, Project administration.

Declaration of competing interest

The authors declare that they have no known competing financial interests or personal relationships that could have appeared to influence the work reported in this paper.

Data availability

The authors do not have permission to share data.

Appendix A

Proof of Lemma 1. The implications of Lemma 1 can be proved through contradiction. Let us first assume that the delay in supplying the per-slot charging demand of EVs is larger than the worst-case delay, i.e., $\left(Z_{d,a}^{\max}+R_{d,a}^{\max}\right)/\varepsilon_{d,a}$. Let us assume that the incoming EV charging demand at the start of the time-horizon is positive, i.e., $I_{d,a}(t)>0$, then, from charging demand backlog update queues as in Eq. (33), we have $R_{d,a}(t+1)>0$ and $R_{d,a}(\tau)>0$ until the time-slot of worst-case delay, i.e., $t+1\leqslant\tau\leqslant t+d_a{}^{\max}$. From the delay-aware virtual queue, as defined in Eq. (35), we have

$$Z_{d,a}(\tau+1)\geqslant Z_{d,a}(\tau)-\left(O_{d,a}\right)+\in_{d,a} \tag{43}$$

Now, summing the above inequality from $(t+1)$ up to $\left(t+d_a{}^{\max}\right)$, we get

$$Z_{d,a}\left(t+d_a^{\max}+1\right)-Z_{d,a}(t+1)\geqslant d_a^{\max}\in_{d,a}-\sum_{\tau=t+1}^{t+d_a^{\max}}O_{d,a}(\tau) \tag{44}$$

Note that $Z_{d,a}\left(t+d_a^{\max}+1\right)\leqslant Z_{d,a}^{\max}$ and $Z_{d,a}(t+1)\geqslant 0$, so we have

$$\sum_{\tau=t+1}^{t+d_a^{\max}}O_{d,a}(t)\geqslant d_a^{\max}\in_{d,a}-Z_{d,a}^{\max} \tag{45}$$

As described above, EV charging demands are fulfilled per user preferences data. It is obvious that, $R_{d,a}(t+1)<R_{d,a}^{\max}$ and assume that the EV charging demand submitted in time-slot t has not been fulfilled until $\left(t+d_a^{\max}\right)$, Therefore, we have $\sum_{\tau=t+1}^{t+d_a^{\max}}O_{d,a}(t)<R_{d,a}^{\max}$. Hence, it is evident from InEq. (45) that $R_{d,a}^{\max}+Z_{d,a}^{\max}>d_a^{\max}\in_{d,a}$. Since, the worst-case delay is $d_a^{\max}=\left(Z_{d,a}^{\max}+R_{d,a}^{\max}\right)/\varepsilon_{d,a}$, then we arrive at the contradiction $R_{d,a}^{\max}+Z_{d,a}^{\max}>Z_{d,a}^{\max}$. Hence, the assumption we made at the start of the proof that the worst-case delay is greater than $d_a^{\max}$ is false.

Appendix B

Proof of Theorem 1. Using the results from the fact $[a-b,0]^2\leqslant(a-b)^2$, and squaring the EV charging demand backlog equation in Eq. (33), delay-aware virtual queue update equation in Eq. (35) and QoP queue in Eq. (36), and rearranging the terms, we get the following bounds

$$\begin{aligned}&1/2\left(M_a(t+1)^2-M_a(t)^2\right)\\&\leqslant 1/2\left(1^2+\phi_a{}^2\right)+M_a(t)\left(\frac{L_a^{curt}(t)}{L_a^{flex}(t)}-\phi_a\right)\end{aligned} \tag{46}$$

$$\begin{aligned}&1/2\left(Z_{d,a}(t+1)^2-Z_{d,a}(t)^2\right)\leqslant(1/2)\left\{\max\left(\varepsilon_{d,a}{}^2,O_{d,a}^{\max}(t)^2\right)\right\}\\&+Z_{d,a}(t)\left\{\varepsilon_{d,a}-O_{d,a}^{\max}(t)\right\}\end{aligned} \tag{47}$$

$$\begin{aligned}&(1/2)\left(R_{d,a}(t+1)^2-R_{d,a}(t)^2\right)\leqslant(1/2)\left\{\left(O_{d,a}^{\max}\right)^2+\left(I_{d,a}^{\max}\right)^2\right\}\\&+R_{d,a}(t)\left\{I_{d,a}^{\max}(t)-O_{d,a}^{\max}(t)\right\}\end{aligned} \tag{48}$$

Now, let us first take the expectation on both sides of the above three inequalities, and then adding the results together will lead to the following inequality.

$$\begin{aligned}&\Delta(\Theta(t))\leqslant\sum_{d\in D_a}\left\{\left(I_{d,a}^{\max}\right)^2+\left(O_{d,a}^{\max}\right)^2\right\}\Big/2\\&\sum_{d\in D_a}\max\left[\left(\varepsilon_{d,a}\right)^2,\left(O_{d,a}^{\max}\right)^2\right]+\left(1+\phi_a{}^2\right)/2\\&+\zeta\sum_{d\in D_a}R_{d,a}(t)\,\mathbb{E}\left[I_{d,a}(t)-O_{d,a}(t)\middle|\,\Theta(t)\right]\\&+\gamma\sum_{d\in D_a}Z_{d,a}(t)\,\mathbb{E}\left[\varepsilon_{d,a}-O_{d,a}(t)\middle|\,\Theta(t)\right]\\&+\xi\sum M_a(t)\,\mathbb{E}\left[\frac{L_a^{curt}(t)}{L_a^{flex}(t)}-\phi_a\middle|\,\Theta(t)\right]\end{aligned} \tag{49}$$

Adding $V\mathbb{E}[C(t)|\,\Theta(t)]$ on both sides of the above inequality will lead to the implications of the Lemma 2 where

$$B=\sum_{d\in D_a}\left\{\begin{matrix}\left(I_{d,a}^{\max}\right)^2+\left(O_{d,a}^{\max}\right)^2+\\\max\left[\left(\varepsilon_{d,a}\right)^2,\left(O_{d,a}^{\max}\right)^2\right]\end{matrix}\right\}\Big/2+\left(1+\phi_a{}^2\right)/2.$$

Appendix C

Proof of Lemma 2. Let us consider the real-time control policy implemented for solving the problem P3 using *Algorithm-1*, and from mean-rate-stability-theorem, as described in Section 3.2.1, recall that all the virtual queues are mean-rate stable. Then from the Lemma 2 it follows that

$$\begin{aligned}&\Delta(\Theta(t))+V\mathbb{E}[C(t)|\,\Theta(t)]\leqslant B\\&+\zeta\sum_{d\in D_a}R_{d,a}(t)\,\mathbb{E}\left[I_{d,a}(t)-O_{d,a}(t)\middle|\,\Theta(t)\right]\\&+\gamma\sum_{d\in D_a}Z_{d,a}(t)\,\mathbb{E}\left[\varepsilon_{d,a}-O_{d,a}(t)\middle|\,\Theta(t)\right]\\&+\xi\sum M_a(t)\,\mathbb{E}\left[\frac{L_a^{curt}(t)}{L_a^{flex}(t)}-\phi_a\middle|\,\Theta(t)\right]\\&+V\mathbb{E}[C(t)|\,\Theta(t)]\leqslant B+V\cdot C^*\end{aligned} \tag{50}$$

Thereafter, applying the Lyapunov per-slot conditional drift and the law of total expectations, it implies that

$$\begin{aligned}&\mathbb{E}[L(\Theta(t+1))-L(\Theta(t))]\\&+V\mathbb{E}[C(t)|\,\Theta(t)]\leqslant B+V\cdot C^*\end{aligned} \tag{51}$$

then, taking the long-term sum on both sides of the above inequality and applying the expectation operator, we get

$$\mathbb{E}\left[L\left(\Theta\left(T\right)\right)-L\left(\Theta\left(0\right)\right)\right] \\ +V\sum_{t=0}^{T-1}\mathbb{E}\left[C\left(t\right)\right]\leqslant BT+C^{*}\cdot VT \tag{52}$$

It can be seen clearly that $L\left(\Theta\left(0\right)\right)=0$ and $L\left(\Theta\left(0\right)\right)=0$, i.e., the conditional drift at the start and the end of the time-horizon are finitely positive. Then the above inequality is divided by VT, and taking the limit of the results to infinity yields the implications of Theorem 1.

Appendix D

Proof of Lemma 3. **a**. Let us first see the case $R_{d,a}\left(t\right)\leqslant V\left\{\max\left(\mu_{a}^{cong}+\mu^{ene}\right)\right\}+I_{d,a}^{\max}, \forall t$. It is obvious before the start of the time-horizon, $R_{d,a}\left(0\right)=0,\ for\ t=0$. Suppose this is also true for the time slot t. Then it can be shown that it is also true for the following time slot, i.e., $t+1$. First evaluate the case when $R_{d,a}\left(t+1\right)\leqslant V\left\{\max\left(\mu_{a}^{cong}+\mu^{ene}\right)\right\}+I_{d,a}^{\max}$, consequently, we have $V\left\{\max\left(\mu_{a}^{cong}+\mu^{ene}\right)\right\}<R_{d,a}\left(t\right)\leqslant V\left\{\max\left(\mu_{a}^{cong}+\mu^{ene}\right)\right\}+I_{d,a}^{\max}$. Since the queues can only grow at most by $I_{d,a}^{\max}$ during a time-slot t, as defined in the queue update equation Eq. (33), therefore, the results also hold for this case. Conversely, $V\left\{\max\left(\mu_{a}^{cong}+\mu^{ene}\right)\right\}<R_{d,a}\left(t\right)\leqslant V\left\{\max\left(\mu_{a}^{cong}+\mu^{ene}\right)\right\}+I_{d,a}^{\max}$. For this case, it can be observed that: $R_{d,a}\left(t\right)+Z_{d,a}\left(t\right)>R_{d,a}\left(t\right)>V\left\{\max\left(\mu_{a}^{cong}+\mu^{ene}\right)\right\}>V\left\{\max\left(\mu_{a}^{cong}+\mu^{ene}\right)\right\}$, so the algorithm shall decide $O_{d,a}\left(t\right)=O_{d,a}^{\max}$. Now, if $R_{d,a}\left(t\right)-O_{d,a}^{\max}>0$, then during the time-slot t, the supplied EV charging demand is $O_{d,a}^{\max}$. Since the incoming EV charging requests $I_{d,a}\left(t\right)$ are upper bounded by $I_{d,a}^{\max}$ (alternatively $I_{d,a}^{\max}\leqslant O_{d,a}^{\max}$), then in the next time-slot, queues cannot grow further, i.e., $R_{d,a}\left(t+1\right)\leqslant R_{d,a}\left(t\right)\leqslant V\left\{\max\left(\mu_{a}^{cong}+\mu^{ene}\right)\right\}+I_{d,a}^{\max}$. Eventually, if $R_{d,a}\left(t\right)-O_{d,a}^{\max}\leqslant 0$, next, from the EV charging demand queue backlog evolution queue, it follows that $R_{d,a}\left(t+1\right)=I_{d,a}\left(t\right)\leqslant I_{d,a}^{\max}$, which is again $\leqslant V\left\{\max\left(\mu_{a}^{cong}+\mu^{ene}\right)\right\}+I_{d,a}^{\max}$. Hence, $R_{d,a}\left(t\right)\leqslant V\left\{\max\left(\mu_{a}^{cong}+\mu^{ene}\right)\right\}+I_{d,a}^{\max}, \forall t$. **b**. The proof for $Z_{d,a}\left(t\right)\leqslant V\left\{\max\left(\mu_{a}^{cong}+\mu^{ene}\right)\right\}+\varepsilon_{d,a}, \forall t$, follows similar procedure and is left out for brevity.

References

[1] Outlook IRENA Global Renewables. Energy transformation 2050. Abu Dhabi, UAE: IRENA; 2020.

[2] Wei Xuan, et al. Two-stage cooperative intelligent home energy management system for optimal scheduling. IEEE Trans Ind Appl 2022;58(4):5423–37. http://dx.doi.org/10.1109/TIA.2022.3172669.

[3] Seal Sayani, Boulet Benoit, Dehkordi Vahid R, Bouffard François, Joos Geza. Centralized MPC for home energy management with EV as mobile energy storage unit. IEEE Trans Sustain Energy 2023;14(3):1425–35. http://dx.doi.org/10.1109/TSTE.2023.3235703.

[4] Haider Sajjad, Walewski John, Schegner Peter, et al. Investigating peer-to-peer power transactions for reducing EV induced network congestion. Energy 2022;254:124317.

[5] Rayati Mohammad, Bozorg Mokhtar, Carpita Mauro, Cherkaoui Rachid. Stochastic optimization and Markov chain-based scenario generation for exploiting the underlying flexibilities of an active distribution network. Sustain Energy Grids Netw 2023;34:100999.

[6] Singh Vikram, et al. Transmission congestion management through sensitivity based rescheduling of generators using improved monarch butterfly optimization. Int J Electr Power Energy Syst 2023;145:108729.

[7] Pal Arnab, Bhattacharya Aniruddha, Chakraborty Ajoy Kumar. Planning of EV charging station with distribution network expansion considering traffic congestion and uncertainties. IEEE Trans Ind Appl 2023.

[8] Alaee Pegah, Bems Julius, Anvari-Moghaddam Amjad. A review of the latest trends in technical and economic aspects of EV charging management. Energies 2023;16(9):3669.

[9] Zadehbagheri Mahmoud, Ildarabadi Rahim, Javadian Abdol Majid. Optimal power flow in the presence of HVDC lines along with optimal placement of FACTS in order to power system stability improvement in different conditions: Technical and economic approach. IEEE Access 2023;11:57745–71. http://dx.doi.org/10.1109/ACCESS.2023.3283573.

[10] Kandpal Bakul, Pareek Parikshit, Verma Ashu. A robust day-ahead scheduling strategy for EV charging stations in unbalanced distribution grid. Energy 2022;249:123737.

[11] García-Muñoz Fernando, Ivanova Anzhelika, Montané Jordi Farré, Serrano Manel, Corchero Cristina. A DSO flexibility platform based on an optimal congestion management model for the European CoordiNet project. Electr Power Syst Res 2023;221:109386.

[12] Narain Aishvarya, Srivastava SK, Singh SN. Congestion management approaches in restructured power system: Key issues and challenges. Electr J 2020;33(3):106715.

[13] Nawaz Arshad, Zhou Min, Wu Jing, Long Chengnian. A comprehensive review on energy management, demand response, and coordination schemes utilization in multi-microgrids network. Appl Energy 2022;323:119596.

[14] Cheng Lilin, Zang Haixiang, Wei Zhinong, Sun Guoqiang. Secure multi-party household load scheduling framework for real-time demand-side management. IEEE Trans Sustain Energy 2022;14(1):602–12.

[15] Babagheibi Mahsa, Jadid Shahram, Kazemi Ahad. Distribution locational marginal pricing for congestion management of an active distribution system with renewable-based microgrids under a privacy-preserving market clearing approach and load models. Sustain Energy Grids Netw 2022;32:100935.

[16] Babagheibi Mahsa, Jadid Shahram, Kazemi Ahad. An incentive-based robust flexibility market for congestion management of an active distribution system to use the free capacity of microgrids. Appl Energy 2023;336:120832.

[17] Zou Luyao, Munir Md Shirajum, Tun Yan Kyaw, Kang Seokwon, Hong Choong Seon. Intelligent ev charging for urban prosumer communities: An auction and multi-agent deep reinforcement learning approach. IEEE Trans Netw Serv Manag 2022;19(4):4384–407.

[18] Amin M Asim, et al. Profit maximization by integrating demand response in multiple vpps optimal scheduling. In: 2022 international conference on electrical engineering and sustainable technologies (ICEEST). IEEE; 2022, p. 1–6.

[19] Li Jiangnan, et al. Energy trading of multiple virtual power plants using deep reinforcement learning. In: 2021 international conference on power system technology (POWERCON). IEEE; 2021, p. 892–7.

[20] Li Zhi, et al. Efficient reactive power control using reinforcement learning under inaccurate power network model. In: 2021 6th international conference on power and renewable energy (ICPRE). IEEE; 2021, p. 350–5.

[21] Liu Shengyuan, Chen Changming, Jiang Yicheng, Lin Zhenzhi, Wang Hongtao, Waseem Muhammad, Wen Fushuan. Bi-level coordinated power system restoration model considering the support of multiple flexible resources. IEEE Trans Power Syst 2022;38(2):1583–95.

[22] Eissa MM. First time real time incentive demand response program in smart grid with "i-energy" management system with different resources. Appl Energy 2018;212:607–21.

[23] Suleman Ahmad, et al. Smart scheduling of EVs through intelligent home energy management using deep reinforcement learning. In: 2022 17th international conference on emerging technologies (ICET). 2022, p. 18–24. http://dx.doi.org/10.1109/ICET56601.2022.10004664.

[24] Singh Shailendra, Pamshetti Vijay Babu, Thakur Amit Kumar, Singh SP, Gooi Hoay Beng. Profit maximization in ADN through voltage control and DR management with networked community micro-grids. IEEE Trans Ind Appl 2023.

[25] Fattaheian-Dehkordi Sajjad, Tavakkoli Mehdi, Abbaspour Ali, Fotuhi-Firuzabad Mahmud, Lehtonen Matti. An incentive-based mechanism to alleviate active power congestion in a multi-agent distribution system. IEEE Trans Smart Grid 2020;12(3):1978–88.

[26] Hu Junjie, Wu Jiechen, Ai Xin, Liu Nian. Coordinated energy management of prosumers in a distribution system considering network congestion. IEEE Trans Smart Grid 2020;12(1):468–78.

[27] Tan Bifei, Chen Haoyong, Zheng Xiaodong, Huang Jianping. Two-stage robust optimization dispatch for multiple microgrids with electric vehicle loads based on a novel data-driven uncertainty set. Int J Electr Power Energy Syst 2022;134:107359.

[28] Jha Sudan, Jha Nishant, Prashar Deepak, Ahmad Sultan, Alouffi Bader, Alharbi Abdullah. Integrated IoT-based secure and efficient key management framework using hashgraphs for autonomous vehicles to ensure road safety. Sensors 2022;22(7):2529.

[29] Huang Shaojun, Wu Qiuwei, Zhao Haoran, Li Canbing. Distributed optimization-based dynamic tariff for congestion management in distribution networks. IEEE Trans Smart Grid 2017;10(1):184–92.

[30] Huang Shaojun, Wu Qiuwei. Dynamic subsidy method for congestion management in distribution networks. IEEE Trans Smart Grid 2016;9(3):2140–51.

[31] Subramanian Vignesh, Das Tapas K, Kwon Changhyun, Gosavi Abhijit. A data-driven methodology for dynamic pricing and demand response in electric power networks. Electr Power Syst Res 2019;174:105869.

[32] Huang Shaojun, Wu Qiuwei, Cheng Lin, Liu Zhaoxi, Zhao Haoran. Uncertainty management of dynamic tariff method for congestion management in distribution networks. IEEE Trans Power Syst 2016;31(6):4340–7.

[33] Subramanian Vignesh, Das Tapas K. A two-layer model for dynamic pricing of electricity and optimal charging of electric vehicles under price spikes. Energy 2019;167:1266–77.

[34] Huang Shaojun, Wu Qiuwei. Real-time congestion management in distribution networks by flexible demand swap. IEEE Trans Smart Grid 2017;9(5):4346–55.
[35] Shen Feifan, Wu Qiuwei, Huang Shaojun, Chen Xinyu, Liu Hui, Xu Yan. Two-tier demand response with flexible demand swap and transactive control for real-time congestion management in distribution networks. Int J Electr Power Energy Syst 2020;114:105399.
[36] Hassan Muhammad Arshad Shehzad, Chen Minyou, Lin Houfei, Ahmed Mohammed Hassan, Khan Muhammad Zeeshan, Chughtai Gohar Rehman. Optimization modeling for dynamic price based demand response in microgrids. J Clean Prod 2019;222:231–41.
[37] Huang Shaojun, Wu Qiuwei, Oren Shmuel S, Li Ruoyang, Liu Zhaoxi. Distribution locational marginal pricing through quadratic programming for congestion management in distribution networks. IEEE Trans Power Syst 2014;30(4):2170–8.
[38] Gu Chenghong, Yan Xiaohe, Yan Zhang, Li Furong. Dynamic pricing for responsive demand to increase distribution network efficiency. Appl Energy 2017;205:236–43.
[39] Abaza A, Azmy Ahmed M. Dynamic pricing for demand-side management within smart grid environment. In: 2016 IEEE international conference on power and energy (PECon). IEEE; 2016, p. 680–5.
[40] Ghazvini Mohammad Ali Fotouhi, Lipari Gianluca, Pau Marco, Ponci Ferdinanda, Monti Antonello, Soares Joao, Castro Rui, Vale Zita. Congestion management in active distribution networks through demand response implementation. Sustain Energy Grids Netw 2019;17:100185.
[41] Yuan Zhao, Hesamzadeh Mohammad Reza. A distributed economic dispatch mechanism to implement distribution locational marginal pricing. In: 2018 power systems computation conference (PSCC). IEEE; 2018, p. 1–7.
[42] Polisetti Karimulla, Kumar Ashwani. Distribution system nodal prices determination for realistic ZIP and seasonal loads: An optimal power flow approach. Proc Technol 2016;25:702–9.
[43] Huang Pei, Xu Tao, Sun Yongjun. A genetic algorithm based dynamic pricing for improving bi-directional interactions with reduced power imbalance. Energy Build 2019;199:275–86.
[44] Limmer Steffen, Rodemann Tobias. Peak load reduction through dynamic pricing for electric vehicle charging. Int J Electr Power Energy Syst 2019;113:117–28.
[45] Qu Zhaoyang, Xu Chuanfu, Yang Fang, Ling Fan, Pirouzi Sasan. Market clearing price-based energy management of grid-connected renewable energy hubs including flexible sources according to thermal, hydrogen, and compressed air storage systems. J Energy Storage 2023;69:107981.
[46] Zhang XiaoWei, Yu Xiaoping, Ye Xinping, Pirouzi Sasan. Economic energy managementof networked flexi-renewable energy hubs according to uncertainty modeling by the unscented transformation method. Energy 2023;278:128054.
[47] Akbari Ehsan, Shabestari Seyed Farzin Mousavi, Pirouzi Sasan, Jadidoleslam Morteza. Network flexibility regulation by renewable energy hubs using flexibility pricing-based energy management. Renew Energy 2023;206:295–308.
[48] Jokar Mohammad Reza, Shahmoradi Saeid, Mohammed Adil Hussein, Foong Loke Kok, Le Binh Nguyen, Pirouzi Sasan. Stationary and mobile storages-based renewable off-grid system planning considering storage degradation cost based on information-gap decision theory optimization. J Energy Storage 2023;58:106389.
[49] Piltan Ghasem, Pirouzi Sasan, Azarhooshang Alireza, Jordehi Ahmad Rezaee, Paeizi Ali, Ghadamyari Mojtaba. Storage-integrated virtual power plants for resiliency enhancement of smart distribution systems. J Energy Storage 2022;55:105563.
[50] Pirouzi Afshin, Aghaei Jamshid, Pirouzi Sasan, Vahidinasab Vahid, Jordehi Ahmad Rezaee. Exploring potential storage-based flexibility gains of electric vehicles in smart distribution grids. J Energy Storage 2022;52:105056.
[51] Dini Anoosh, Hassankashi Alireza, Pirouzi Sasan, Lehtonen Matti, Arandian Behdad, Baziar Ali Asghar. A flexible-reliable operation optimization model of the networked energy hubs with distributed generations, energy storage systems and demand response. Energy 2022;239:121923.
[52] Yuan Quan, Ye Yujian, Tang Yi, Liu Yuanchang, Strbac Goran. A novel deep-learning based surrogate modeling of stochastic electric vehicle traffic user equilibrium in low-carbon electricity–transportation nexus. Appl Energy 2022;315:118961.
[53] Jafarian Matin, Scherpen Jacquelien MA, Loeff Kees, Mulder Machiel, Aiello Marco. A combined nodal and uniform pricing mechanism for congestion management in distribution power networks. Electr Power Syst Res 2020;180:106088.
[54] Tarashandeh Nader, Karimi Ali. Utilization of energy storage systems in congestion management of transmission networks with incentive-based approach for investors. J Energy Storage 2021;33:102034.
[55] Kumar Nishant, Singh Bhim, Panigrahi Bijaya Ketan. Voltage sensorless based model predictive control with battery management system: for solar PV powered on-board EV charging. IEEE Trans Transp Electrif 2022.
[56] Sohail Abeer, Khan Rashna, Mukhtar Syed Hammad, Najeeb Aiman, Usman Ahmad. Effects of uncoordinated electric vehicle charging on a distribution network. In: 2022 19th international Bhurban conference on applied sciences and technology (IBCAST). IEEE; 2022, p. 591–7.
[57] Oureilidis Konstantinos, Malamaki Kyriaki-Nefeli, Gallos Konstantinos, Tsitsimelis Achilleas, Dikaiakos Christos, Gkavanoudis Spyros, Cvetkovic Milos, Mauricio Juan Manuel, Maza Ortega Jose Maria, Ramos Jose Luis Martinez, et al. Ancillary services market design in distribution networks: Review and identification of barriers. Energies 2020;13(4):917.
[58] Esmat Ayman Adel Salaheldin. Flexibility market for congestion management in smart grids. 2019.
[59] Zhou Yaqin, Yau David KY, You Pengcheng, Cheng Peng. Optimal-cost scheduling of electrical vehicle charging under uncertainty. IEEE Trans Smart Grid 2017;9(5):4547–54.
[60] Liu Zhaoxi, Wu Qiuwei, Oren Shmuel S, Huang Shaojun, Li Ruoyang, Cheng Lin. Distribution locational marginal pricing for optimal electric vehicle charging through chance constrained mixed-integer programming. IEEE Trans Smart Grid 2016;9(2):644–54.
[61] Linna NI, Fushuan WEN, Weijia LIU, Jinling MENG, Guoying LIN, Sanlei DANG. Congestion management with demand response considering uncertainties of distributed generation outputs and market prices. J Mod Power Syst Clean Energy 2017;5(1):66–78.
[62] Amin M Asim, Suleman Ahmad, Waseem Muhammad, Iqbal Taosif, Aziz Saddam, Faiz Muhammad Talib, Zulfiqar Lubaid, Saleh Ahmed Mohammed. Renewable energy maximization for pelagic islands network of microgrids through battery swapping using deep reinforcement learning. IEEE Access 2023.
[63] Zhu Dafeng, Yang Bo, Liu Qi, Ma Kai, Zhu Shanying, Ma Chengbin, Guan Xinping. Energy trading in microgrids for synergies among electricity, hydrogen and heat networks. Appl Energy 2020;272:115225.
[64] Zhu Hailing, Ouahada Khmaies. A distributed real-time control algorithm for energy storage sharing. Energy Build 2021;230:110478.
[65] Liu Nian, Yu Xinghuo, Fan Wei, Hu Cungang, Rui Tao, Chen Qifang, Zhang Jianhua. Online energy sharing for nanogrid clusters: A Lyapunov optimization approach. IEEE Trans Smart Grid 2017;9(5):4624–36.
[66] He Huaiwen, Shen Hong. Minimizing the operation cost of distributed green data centers with energy storage under carbon capping. J Comput System Sci 2020.
[67] Yan Jie, Menghwar Mohan, Asghar Ehtisham, Panjwani Manoj Kumar, Liu Yongqian. Real-time energy management for a smart-community microgrid with battery swapping and renewables. Appl Energy 2019;238:180–94.
[68] Wang Guofeng, Xu Chongbo, Hu Chengpeng, Yang Xiaodong, Zhang Youbing. An online energy flow control strategy for regional integrated energy system. In: 2020 IEEE power & energy society general meeting (PESGM). IEEE; 2020, p. 1–5.
[69] Neely Michael J. Stochastic network optimization with application to communication and queueing systems. Synth Lect Commun Netw 2010;3(1):48.
[70] Shi Guoqing, Zheng Xiaojian, Song Fangfang. Estimating elasticity for residential electricity demand in China. Sci World J 2012;2012.
[71] Lee Henry, Clark Alex. Charging the future: Challenges and opportunities for electric vehicle adoption. 2018.
[72] EnergyOnline CAISO real-time price. 2022, http://www.energyonline.com/Data/GenericData.aspx?DataId=19&CAISO__Real-time_Price. Accessed: 2022-08-30.
[73] CVX MATLAB software for disciplined convex programming. 2022, http://cvxr.com/cvx/. Accessed: 2022-08-30.
[74] Gumpu Srinivasulu, Pamulaparthy Balakrishna, Sharma Ankush. Review of congestion management methods from conventional to smart grid scenario. Int J Emerg Electr Power Syst 2019;20(3).
[75] Holjevac Ninoslav, Baškarad Tomislav, Đaković Josip, Krpan Matej, Zidar Matija, Kuzle Igor. Challenges of high renewable energy sources integration in power systems—The case of Croatia. Energies 2021;14(4):1047.